

Ritz variational principle for collective diffusion in an adsorbate on a non-homogeneous substrate

Magdalena A. Załuska-Kotur*

*Institute of Physics, Polish Academy of Sciences, Aleja Lotników 32/46, 02-668 Warsaw, Poland
and Faculty of Mathematics and Natural Sciences, Cardinal Stefan Wyszyński University, Dewajtis 5, 01-815 Warsaw, Poland*

Zbigniew W. Gortel†

Department of Physics, University of Alberta, Edmonton, Alberta, Canada T6G 2J1

(Received 1 August 2007; revised manuscript received 6 September 2007; published 3 December 2007)

A systematic approach on collective diffusion in an interacting lattice gas adsorbed on a non-homogeneous substrate is formulated. It is based on a variational Ritz procedure of determining a diffusive eigenvalue of a transition rate matrix describing microscopic kinetics of particle migration processes in the system. Form of a trial eigenvector and a choice of variational parameters are discussed and justified on physical grounds. Reed-Ehrlich factorization of the collective diffusion coefficient into the thermodynamic and kinetic factors is explicitly shown to emerge naturally from the variational approach, and closed expressions for both factors are derived. Validity of the approach is tested by applying it to the simplest case of diffusion of noninteracting adparticles across steps on a stepped substrate (modeled by a Schwoebel barrier). The coverage dependence of collective diffusion coefficient, obtained in an algebraic form, agrees very well with the results of Monte Carlo simulations. It is demonstrated that the results obtained provide a substantial improvement over the mean-field theory results for the same system. Generalizations necessary to include interparticle interactions are listed and discussed.

DOI: [10.1103/PhysRevB.76.245401](https://doi.org/10.1103/PhysRevB.76.245401)

PACS number(s): 66.30.Pa, 02.50.Ga, 66.10.Cb, 68.43.Jk

I. INTRODUCTION

The collective or chemical diffusion of adsorbed species involves jumps of interacting particles from one binding site to another. From a perspective of a theorist, it is a complicated many-body problem of diffusion in low-dimensional systems to which a variety of approaches were applied ranging from analytic ones based on master, Fokker-Planck, and Kramers equations to numerical Monte Carlo or molecular dynamics simulations. An important background is provided by the works of Reed and Ehrlich,¹ an early summary by Gomer,² and recent reviews by Danani *et al.*³ and Ala-Nissila *et al.*⁴ Relevant analytic results for some generic simple models are collected by Haus and Kehr,⁵ and interrelations between different statistical descriptions of these processes have been reviewed by Allnatt and Lidiard.⁶

Our interest is the coverage dependence of the collective diffusion coefficient in a kinetic lattice gas model. We mention here a number of theoretical works devoted to it due to their relevance to this work and to our earlier efforts.⁷⁻¹¹ One of the earliest seems a linear response theory approach by Zwerger,¹² which allowed him to derive analytic expressions for the coverage dependent collective diffusion coefficient $D(\theta)$ for a one-dimensional (1D) lattice gas with nearest-neighbor (NN) and next-nearest-neighbor (NNN) interactions. Kreuzer and Zhang, using a version of the kinetic lattice gas model which they developed earlier to study thermal desorption kinetics,^{13,14} investigated $D(\theta, T)$ (with T being temperature) in a 1D lattice gas with NN interactions and different models of microscopic kinetics.¹⁵ Starting from the master equation describing kinetics of microscopic states of the system, the equation for the time evolution of the local density was derived in terms of correlation functions which

were then approximately evaluated by applying a gradient expansion. Somewhat earlier, an exact analysis of the short time transients and diffusion on finite 1D chains of adsorption sites with NN interactions between particles was reported.¹⁶ This time, the analysis was based on the microscopic master equation directly by investigating the eigenvalues of the associated rate matrix. Crucial for this approach was distributing all possible microstates among equivalence classes of microstates with identical, modulo periodic boundary conditions, relative positions of particles (i.e., all microstates within the class have an identical geometrical pattern of occupied sites). The same idea is at the basis of the approach described in this paper, as well as in all our earlier work^{7-11,17} on diffusion in the interacting lattice gas.¹⁸

Our goal is to develop a systematic approach on collective diffusion of interacting particles on a one-dimensional periodic lattice of adsorption sites with varying binding energies (potential well depths) and varying barrier heights between the sites, i.e., on a non-homogeneous but periodic substrate. The approach is based on the application of Ritz variational principle to evaluate approximately the smallest (in the absolute value sense) eigenvalue of a rate matrix describing kinetics of microscopic states of the interacting lattice gas system. The method evolved from the approach formulated first in Ref. 7, refined later in Refs. 8-11, and applied recently¹⁷ to account for low-temperature ultrafast mobility in Pb/Si(111) due to long-range interparticle interactions.

To summarize that in what follows, we note that as in any variational approach, a crucial initial step is a proposition of a trial vector approximating best the true *diffusive eigenvector* of the rate matrix corresponding to its *diffusive eigenvalue* $-\lambda_D$ from which the collective diffusion coefficient can be directly extracted in the long wavelength ($k \rightarrow 0$) limit:

$$D = \lim_{k \rightarrow 0} \frac{\lambda_D(k)}{k^2}. \quad (1)$$

The diffusive eigenvalue, vanishing in the long wavelength limit [as seen from Eq. (1)], is the one with the smallest absolute value among all eigenvalues of the rate matrix (all eigenvalues of the rate matrix are negative). This property makes the problem of its calculation suitable for the variational approach. The major difference between the standard variational approach from quantum mechanics textbooks and that used for the rate matrix is that the latter is not a Hermitian matrix which requires a careful reexamination of the Ritz principle. The other difference is technical: we usually do not possess intuitions serving as a guide in selecting a candidate for the trial eigenvector (in contrast to the ground state wave functions for which our intuitions are better developed). Its selection, ideally guided by physical intuition, is aided by the structure of the eigenvector for exactly solvable cases. Such selection must result in the trial eigenvalue which vanishes in the long wavelength limit. Ideally, the candidate eigenvector should depend on several free parameters which can be adjusted to minimize the absolute value of the calculated eigenvalue. In all applications so far,⁷⁻¹¹ no variational parameters were introduced, severely restricting a class of problems to which the variational method could be applied. This deficiency will be removed in this work.

The remainder of the paper is organized as follows. In Sec. II, the system of interest is defined and the theory developed in Refs. 7, 8, and 11 is summarized and generalized for the case of a non-homogeneous substrate. In particular, the microscopic rate matrix is defined toward the end of Sec. II A and its exact properties are summarized in Sec. II B. In Sec. II C, the trial diffusive eigenvector and variational parameters are proposed and the choice of its form is rationalized. Diffusion coefficient is shown in Sec. II D to be a product of two factors, which are shown to be exactly the factors in the Reed-Ehrlich factorization.^{1,19} The results of this section provide a general framework which can be used for a variety of applications for systems with different types of substrate non-homogeneity, different interparticle interactions, and different microscopic kinetics. The expressions provided can be used directly for systems with NN interactions and phase correlations, but generalizations for NNN interactions and phase correlations and beyond are straightforward. In Sec. III, the method is applied for the simplest possible nontrivial case of diffusion of noninteracting particles across steps along stepped substrate, the latter being modeled by a Schwoebel barrier.^{20,21} The absence of interactions allows for the entire calculation to be done analytically for arbitrary step lengths and the result for $D(\theta)$ is algebraic. The model system is specified here by two parameters, one fully specifying the equilibrium properties [r , cf. Eq. (38b)] and the other specifying the microscopic migration kinetics [γ , cf. Eq. (38a)]. Types of $D(\theta)$ dependence are presented and discussed in Sec. IV, where a comparison with Monte Carlo simulation results of diffusion for selected systems and a comparison with an earlier investigation of diffusion on a stepped surface by Merikoski and Ying^{22,23} are also provided. Section V is devoted to a preliminary discussion of

generalizations necessary to include interparticle interactions. This work is in progress and will be reported on in the near future. The paper is briefly summarized in Sec. VI.

II. THEORY

A. Model and definitions

We envisage a system of N particles distributed over a substrate being a periodic lattice consisting of L identical elementary cells labeled $j=0, 1, 2, \dots, L-1$. Each elementary cell consists of $n+1$ lattice sites S_ℓ labeled $\ell=0, 1, 2, \dots, n$, separated by a distance a . The length of the unit cell—the translational period of the lattice—is $\mathcal{A}=(n+1)a$ and the length of the substrate is $\mathcal{A}L$. We have

$$\cdots S_n \underbrace{\left[S_0 S_1 S_2 \cdots S_\ell \cdots S_{n-2} S_{n-1} S_n \right]}_{j\text{th cell}} S_0 \cdots, \quad (2)$$

Each site can bind an adsorbed particle with different energy, and the barrier heights between adjacent potential wells may be different for each pair of neighboring sites. Obviously, binding energy at a site S_ℓ within j th unit cell and the surrounding potential barrier heights depend on ℓ (i.e., the position within the elementary cell) but not on j (the position of the cell itself). Applying results of this work, however, we will let, at most, the barrier height between S_n and S_0 and the well depth of S_0 be different from all the remaining ones. This is known as a Schwoebel barrier used to model migration on stepped surfaces.^{20,21} With the origin of the coordinate system at the ($j=0, \ell=0$) site, the absolute position of a general (j, ℓ) (i.e., S_ℓ site within the j th elementary cell) is $j\mathcal{A} + \ell a$. The index $\ell=0, 1, 2, \dots, n$ labels the sites within a unit cell; so, if an integer needs to be added to (subtracted from) it and results in an integer larger than n (smaller than 0), then $n+1$ must be subtracted from (added to) the result to get the actual index ℓ' of the site within a neighboring elementary cell. We refer to a as a *fractional* lattice constant to distinguish it from the proper lattice constant $\mathcal{A}=(n+1)a$. Periodic boundary condition is imposed allowing us to consider all $(n+1)L$ sites (L elementary cells) to be arranged along a circumference of a circle of length $L\mathcal{A}$. Two possible directions along the line are referred to either as clockwise (from left to right) or counterclockwise (from right to left). In the wave number (k) domain, the periodic boundary implies that the condition

$$e^{ik\mathcal{A}L} = 1 \quad (3)$$

must be used in the calculations before the long wavelength limit $k\mathcal{A} \ll 1$ is applied.

We treat diffusion within an adsorbate using a kinetic lattice gas model. Basic assumptions are standard: kinetics of the microstates of the lattice gas is due to stochastic hopping of particles to neighboring sites, only one particle in the gas hops at any given instant, an average residence time of particles at the adsorption sites is much longer than the transit time between the sites, and the transition rates of these hops depend on the potential energy landscape experienced by the hopping particle and its modifications due to instantaneous

particle-particle interactions. This allows us to start from the set of the Markovian master rate equations for the probabilities $P(\{c\}, t)$ that a microscopic *microstate* $\{c\}$ of a lattice gas occurs at time t ,

$$\frac{d}{dt}P(\{c\}, t) = \sum_{\{c'\}} [W(\{c\}, \{c'\})P(\{c'\}, t) - W(\{c'\}, \{c\})P(\{c\}, t)]. \quad (4)$$

$\{c\}$ is understood as a set of variables specifying which particular sites in the lattice are occupied and which are not. No adsorption site can be doubly occupied. $W(\{c\}, \{c'\})$ is a transition probability per unit time (transition rate) that the microstate $\{c'\}$ changes into $\{c\}$ due to a jump of a particle from an occupied site to an unoccupied neighboring site. A pair of microstates $\{c\}$ and $\{c'\}$ between which such transition may occur will be referred to as a *linked* pair of microstates [i.e., $W(\{c\}, \{c'\}) \neq 0$ only when $(\{c\}, \{c'\})$ is a linked pair of microstates]. In practice, the rate $W(\{c\}, \{c'\})$ does not depend on all variables needed to specify such a pair. In the absence of interparticle interactions, the rate depends only on the local potential energy landscape experienced by the hopping particle; for example, for thermally activated jumps, it depends on the difference between the potential energy of the particle at the top of the potential energy barrier between the sites involved and that at the initial site. It does not depend on that in which elementary cell jump occurs. Therefore, if the $\{c'\} \rightarrow \{c\}$ transition involves a particle jump from site S_ℓ to $S_{\ell+1}$, then $W(\{c\}, \{c'\})$ has a value denoted $\dot{W}_{\ell+1}^\ell$, where the circle above W refers to the noninteracting case. For short-range interactions between particles, the rate $W(\{c\}, \{c'\})$ depends not only on the local potential energy landscape but also on the occupation state of the neighboring sites because, in the above example, interactions modify the binding energy at the initial site as well as the potential energy at the top of the barrier. Still, $W(\{c\}, \{c'\})$ depends only on a relatively few variables needed to specify the linked pair of microstates and the rate will be denoted $W_{\ell+1}^\ell(\dots)$, where the ellipses stand for all necessary occupation numbers of neighboring sites whose occupation influences the rate. In fact, apart from zero, $W(\{c\}, \{c'\})$ can only assume four different values in case of $n=0$ (one site per unit cell) when only the nearest-neighbor interactions are important.⁷ For a non-homogeneous substrate (i.e., with several nonequivalent sites and/or barriers per unit cell), the number of possible rates is correspondingly larger.

Following Ref. 7, we identify a microstate $\{c\}$ by selecting one particle as a *reference particle* and specify positions of all remaining $N-1$ particles with respect to it. If the position of the reference particle is $X+a\ell_0$, where $X=Aj_0$ is a position of the elementary cell in which it resides, then a microstate $\{c\}$ may be identified by the following set of $N+1$ numbers:

$$c = [X; \ell_0; m_1, m_2, \dots, m_{N-1}] \equiv [X; \{m\}], \quad (5)$$

where m_s is an integer indicating how far, in units of the fractional lattice constant a , is the s th particle ($s=1, 2, \dots, N-1$) from the reference particle (sometimes, it is conve-

nient to allow $s=0$ with $m_0=0$ to label the reference particle itself and its position). The set of N integers, $\{m\} = [\ell_0; m_1, m_2, \dots, m_{N-1}]$, is referred to as a *configuration*—it accounts for the relative arrangement of particles in a given microstate $\{c\}$. Note the different meanings attached to terms microstate and configuration in this convention. In order to avoid the influence of the boundaries, we let $j_0 = 0, \pm 1, \pm 2, \dots, \pm \infty$ and impose the already mentioned periodic boundary condition allowing elementary cells separated by $\mathcal{A}L \times \text{integer}$ to represent the same cell. If the reference particle is selected as the leftmost one in the system, then the integers $s=1, 2, \dots, N-1$ label the remaining ones in order in which they are encountered going from the reference particle in the clockwise (right) direction. Consequently, all m_s 's are positive integers satisfying the ordering condition

$$1 \leq m_1 < \dots < m_s < \dots < m_{N-1} \leq (n+1)L-1, \quad (6)$$

which assures that the shortest and longest distances between any two particles are a and $[(n+1)L-1]a=L\mathcal{A}-a$, respectively. For the s th particle to the right of the reference one, residing at site S_ℓ within j_s th elementary cell, we have $m_s = (n+1)(j_s - j_0) + (\ell_s - \ell_0)$. Note that for a specified linked pair of configurations, $(\{m\}, \{m'\})$, the site type S_ℓ where the hopping particle initially resides, as well as the occupation state of each site around it, is uniquely specified. Consequently, the jump rate (in either direction) in this configuration is uniquely specified by specifying the linked pair $(\{m\}, \{m'\})$: the transition rate $W(\{c\}, \{c'\})$ depends only on $(\{m\}, \{m'\})$, but it does not depend on the actual position of the elementary cells, X and X' , of the reference particle after and before the transition (X and X' must not be the same when the reference particle itself performs the jump). Therefore, $W(\{c\}, \{c'\}) \equiv W_{\{m\}, \{m'\}}$, which allows us to take advantage of the lattice periodicity to take a lattice Fourier transform,

$$P_{\{m\}}(k, t) = \sum_X e^{ikX} P_{\{m\}}(X, t) = \sum_{j_0=-\infty}^{+\infty} e^{ikAj_0} P_{\{m\}}(Aj_0, t), \quad (7)$$

of both sides of the rate equations [Eq. (4)]. $P_{\{m\}}(X, t)$ stands here for $P(\{c\}=[X; \{m\}], t)$. It is convenient to treat $P_{\{m\}}(k, t)$ as an $\{m\}$ th component of a one-column array $\mathbf{P}(k, t)$ with a macroscopic number of components—each component corresponds to an admissible microscopic configuration of the system. The Fourier-transformed rate equations can be written in a compact form,

$$\frac{d}{dt}\mathbf{P}(k, t) = \mathbb{M}(k) \cdot \mathbf{P}(k, t), \quad (8)$$

where “ \cdot ” denotes multiplication following usual “rows times columns” multiplication rules. Some elements of a square *rate matrix* contain a k -dependent phase factor $\exp(\pm ik\mathcal{A})$ [cf. Eqs. (9) and (10) to follow], because a jump of a reference atom may convert a configuration tied to a lattice cell X into the one tied to $X \mp \mathcal{A}$ [for more details, cf. Eq. (11) with the discussion following it in Ref. 8 and Appendix A of Ref. 7].

Eigenvalues of the rate matrix account for the temporal decay of a k th Fourier component of a density fluctuation from equilibrium. The one vanishing like k^2 in the long wavelength limit, $-\lambda_D(k)$, is referred to as diffusive eigenvalue and yields the collective diffusion coefficient as already implied in Eq. (1). The corresponding eigenvector of $\mathbb{M}(k)$ is referred to as the diffusive eigenvector.

B. Rate matrix: Exact properties

The rate matrix has several mathematical properties essential for the development of the method. They have been derived in Appendix A of Ref. 7, and in what follows, we list the most important ones.

The matrix elements of $\mathbb{M}(k)$ can be expressed in terms of the original rates $W_{\{m\},\{m'\}}$,

$$M_{\{m\},\{m'\}}(k) = W_{\{m\},\{m'\}}(k) - \delta_{\{m\},\{m'\}} \sum_{\{m''\}} W_{\{m''\},\{m\}}, \quad (9)$$

where $\delta_{\{m\},\{m'\}}$ is a Kronecker delta equal to 1 only when all indices in $\{m\}$ are equal to the corresponding ones in $\{m'\}$ and

$$W_{\{m\},\{m'\}}(k) = F_{\{m\},\{m'\}}(k) W_{\{m\},\{m'\}}. \quad (10)$$

Note that for $\{m\}=\{m'\}$, only the second term in Eq. (9) contributes because, evidently, $W_{\{m\},\{m\}}=0$. The k -dependent factor F is usually equal to 1 except for $\{m'\} \rightarrow \{m\}$ transitions involving a jump of the reference atom across a boundary between neighboring elementary cells. Then, $F_{\{m\},\{m'\}}(k) = \exp(\mp ikA)$ (the sign depends on the direction of the jump). The important point is that $F_{\{m\},\{m'\}}(0)=1$ and that its absolute value for any k is equal to 1.

The rates W satisfy the detailed balance condition which is inherited by the rate matrix $\mathbb{M}(k)$ as follows:

$$M_{\{m\},\{m'\}}(k) P_{\{m'\}}^{\text{eq}} = M_{\{m'\},\{m\}}^*(k) P_{\{m\}}^{\text{eq}}. \quad (11)$$

Here, $P_{\{m\}}^{\text{eq}}$ is the equilibrium probability of configuration $\{m\}$. Consequently, $\mathbb{M}(k)$ is not a Hermitian matrix but there exists a real, diagonal, k -independent transformation matrix with diagonal matrix elements $1/\sqrt{P_{\{m\}}^{\text{eq}}}$ which transforms it into a Hermitian matrix. Consequently, the eigenvalues of $\mathbb{M}(k)$ are real, and, using the detailed balance condition, one can show that all of them are negative reflecting the fact that all deviations from equilibrium decay with time. Non-Hermiticity of $\mathbb{M}(k)$ implies that its left eigenvector, say, $\tilde{\mathbf{e}}(k)$, is not the Hermitian conjugate of the corresponding right eigenvector $\mathbf{e}(k)$ (left eigenvectors, with a tilde above the symbol, are one-row rather than one-column arrays). Detailed balance condition, however, implies that the corresponding components of the left and right eigenvectors are related to each other through the equilibrium probabilities:

$$e_{\{m\}}(k) = P_{\{m\}}^{\text{eq}} \tilde{e}_{\{m\}}^*(k), \quad (12)$$

where “*” denotes complex conjugation.

It follows from Eq. (9) that

$$\sum_{\{m\}} M_{\{m\},\{m'\}}(0) = 0, \quad (13)$$

which is an expression of the particle conservation. Namely, written as $\tilde{\mathbf{e}}^D(0) \cdot \mathbb{M}(0) = 0$, it implies that there exists an eigenvalue $-\lambda_D(k)$, exactly the one referred to as the diffusive eigenvalue, which tends to zero in the long wavelength ($k \rightarrow 0$) limit and that all components of the corresponding diffusive left eigenvector $\tilde{\mathbf{e}}^D(k)$ become equal to each other in the same limit, say, $\tilde{e}_{\{m\}}^D(0) = 1$ for all $\{m\}$'s. Components of the diffusive right eigenvector are then, according to Eq. (12), $e_{\{m\}}^D(0) = P_{\{m\}}^{\text{eq}}$ in this limit, i.e.,

$$\mathbb{M}(0) \cdot \mathbf{P}^{\text{eq}} = 0. \quad (14)$$

Proof of the variational Ritz principle usually formulated for Hermitian operators (matrices) can be generalized to a non-Hermitian matrix $-\mathbb{M}(k)$ satisfying the detailed balance condition (11). Namely, for any trial left eigenvector $\tilde{\boldsymbol{\phi}}$ (possibly k dependent) and its right eigenvector counterpart $\boldsymbol{\phi}$ with components

$$\phi_{\{m\}} = P_{\{m\}}^{\text{eq}} \tilde{\phi}_{\{m\}}^*, \quad (15)$$

the following inequality holds:

$$\lambda_D^{\text{var}} \equiv \frac{\tilde{\boldsymbol{\phi}} \cdot [-\mathbb{M}(k)] \cdot \boldsymbol{\phi}}{\tilde{\boldsymbol{\phi}} \cdot \boldsymbol{\phi}} \geq \lambda_D(k), \quad (16)$$

provided $P_{\{m\}}^{\text{eq}}$'s are true equilibrium probabilities determined by Eq. (14). Here, $\lambda_D(k)$ is the smallest eigenvalue of $-\mathbb{M}(k)$, which, for small enough k , is just the diffusive eigenvalue. Therefore, although there is a freedom in selecting the trial left eigenvectors, the calculated λ_D^{var} approximates the true diffusive eigenvalue from above only when true equilibrium probabilities $P_{\{m\}}^{\text{eq}}$ are employed in the calculation; our confidence in the accuracy of the calculated dynamic quantity (the collective diffusion coefficient) hinges on our ability to calculate the static properties of the system exactly. Inequality (16) allows one to select parameter dependent trial left eigenvectors and then minimize the result with respect to these parameters to get the best possible approximation for $\lambda_D(k)$.

We see from Eq. (16) that λ_D^{var} is a ratio,

$$\lambda_D^{\text{var}} = \frac{\mathcal{M}(k)}{\mathcal{N}(k)}, \quad (17)$$

of the “expectation value” numerator,

$$\mathcal{M}(k) = \sum_{\{m\},\{m'\}}^{\text{norep}} P_{\{m'\}}^{\text{eq}} W_{\{m\},\{m'\}} |F_{\{m\},\{m'\}}(k) \tilde{\phi}_{\{m'\}}^*(k) - \tilde{\phi}_{\{m\}}^*(k)|^2, \quad (18)$$

to the “normalization” denominator,

$$\mathcal{N}(k) = \sum_{\{m\}} P_{\{m\}}^{\text{eq}} |\tilde{\phi}_{\{m\}}(k)|^2. \quad (19)$$

Equations (9), (10), and (15) have been used to get the final expression for the numerator in Eq. (18). The detailed balance condition (11) allowed us to account in each term the

sum corresponding to a linked pair of configurations $(\{m\}, \{m'\})$ for transitions from $\{m'\}$ to $\{m\}$ and back. Each such pair should appear in the sum only once [as indicated by the comment “no rep” above the sum in Eq. (18)] in order to avoid double counting.

Note that both $\mathcal{M}(k)$ and $\mathcal{N}(k)$ are thermal equilibrium averages of certain microscopic quantities. Although the system considered has fixed size (L) and contains fixed number of particles (N), the averages can be evaluated using any convenient statistical ensemble.

C. Trial eigenvector

Selecting the trial left eigenvector of the rate matrix, we are guided by the results for the case for which the eigenvector can be found exactly: a system of noninteracting particles (except for hard core repulsion preventing from more than one to be adsorbed at any adsorption site) moving on a homogeneous substrate, i.e., a periodic lattice of identical adsorption sites separated by identical potential energy barriers. In the language of the present model, we have $n=0$ (one site per elementary cell), $\mathcal{A}=a$, and only one jump rate (say, \dot{W}). The diffusive eigenvalue does not depend on coverage;²⁴ we have $\lambda_D^{\text{eq}}(k) = 4\dot{W} \sin^2(ka/2)$ yielding the collective diffusion coefficient $\dot{D} = \dot{W}a^2$. The rate matrix $\dot{M}(k)$ is Hermitian in this case, and all microscopic configurations are equally probable (all $P_{\{m\}}^{\text{eq}}$'s can be set to, say, 1). Components of the left diffusive eigenvector $\tilde{e}^D(k)$ are⁷

$$\begin{aligned} \tilde{e}_{m_1, m_2, \dots, m_{N-1}}^D(k) &\equiv \tilde{e}_{\{m\}}^D(k) = 1 + \sum_{s=1}^{N-1} e^{ikam_s} \\ &= 1 + e^{ikam_1} + e^{ikam_2} + \dots + e^{ikam_{N-1}}, \end{aligned} \quad (20)$$

and the components of the corresponding right eigenvector are obtained by complex conjugation. Note that for $n=0$, the label ℓ_0 is superfluous in the specification of configuration $\{m\}$ [cf. Eq. (5)]. Several comments are noteworthy. (i) The eigenvector is just a sum of phase factors associated with occupied sites. (ii) A site occupied in configuration $\{m\}$ by s th particle has a phase kam_s relative to the phase of the site occupied by the reference particle. (iii) All components of the diffusive left eigenvector become equal to each other in the long wavelength limit. This follows from the particle number conservation as explained in the paragraph containing Eqs. (13) and (14).

These three properties provide a guide in selecting trial left eigenvectors for all cases considered. For a non-homogeneous substrate with arbitrary n , interacting or not, we propose that the trial left eigenvector has $\{m\}$ th component equal, like in Eq. (20), to a sum of phase factors associated with all occupied sites in configuration $\{m\}$:

$$\tilde{\phi}_{\{m\}}(k) = e^{ika(\delta_{\ell_0} + \Delta_{\ell_0})} + \sum_{s=1}^{N-1} e^{ika(m_s + \delta_{\ell_s} + \Delta_{\ell_s})}. \quad (21)$$

Note that a is now the fractional lattice constant in contrast to that in Eq. (20). The phase contributed by the s th particle

is now determined not only by its distance am_s from the reference particle. It receives two additional distinct contributions δ_{ℓ_s} and Δ_{ℓ_s} which play a role of the variational parameters allowing us to minimize $\lambda_D^{\text{var}}(k)$. Both depend on position $a\ell_s$ within an elementary cell of site S_{ℓ_s} at which the s th particle resides. The first one, δ_{ℓ_s} , called the *geometrical phase*, does not depend on the presence of other particles in the system. Without sacrificing generality of the approach, one can select $\delta_0=0$, meaning that geometrical phases are counted with respect to that of the S_0 site. The other phase, Δ_{ℓ_s} , called the *correlational phase*, is introduced to account for correlations between the s th particle and all the remaining ones and, in principle, it depends on the state of occupation of all sites in the system. Such general dependence is intractable, so we assume that it is sensitive to the occupation of sites nearest to S_{ℓ_s} only:

$$\Delta_{\ell_s} = \begin{cases} \Delta_{\ell_s}^L & \text{if site } S_{\ell_{s-1}} \text{ is occupied} \\ \Delta_{\ell_s}^R & \text{if site } S_{\ell_{s+1}} \text{ is occupied} \\ \Delta_{\ell_s}^L + \Delta_{\ell_s}^R & \text{if both are occupied} \\ 0 & \text{otherwise.} \end{cases} \quad (22)$$

Effectively, we admit short-range correlations only for correlational phases. It follows then that $\Delta_{\ell_s}^L = -\Delta_{\ell_s}^R$ when the short-range energy landscape is symmetric with respect to site S_{ℓ_s} , i.e., when barriers on its both sides as well as the binding energy of both sites behind them are identical. Summarizing, a phase associated with each particle in the system depends on (i) the distance of the particles from the reference particle, (ii) an address within the elementary cell of the site which it occupies, and (iii) state of occupation of the sites adjacent to it.

We note in passing that in a more sophisticated version of the theory, one might not assume the additivity of the correlational phases embodied in the third line of Eq. (22). This would result in an extra variational parameters, say, $\Delta_{\ell_s}^{LR}$, not necessarily equal to $\Delta_{\ell_s}^L + \Delta_{\ell_s}^R$. This possibility was not explored in this work.

D. Diffusion coefficient

We are now ready to simplify expressions for the numerator $\mathcal{M}(k)$ [Eq. (18)] and the denominator $\mathcal{N}(k)$ [Eq. (19)] of the trial diffusive eigenvalue. We will show that the calculation of the numerator can be reduced to the calculation of four-site correlation functions, while for the denominator, two-site correlation functions are needed. In fact, we demonstrate in Appendix A that the dependence of the diffusion denominator $\mathcal{N}(k)$ on variational parameters δ_{ℓ_s} and Δ_{ℓ_s} can be ignored in the long wavelength limit and that

$$\lim_{k \rightarrow 0} \frac{\mathcal{N}(k)}{N} = \left[\left(\frac{\partial(\mu/k_B T)}{\partial \ln \theta} \right)_{L,T} \right]^{-1} = k_B T \theta \kappa_T, \quad (23a)$$

or, equivalently,

$$\mathcal{N}(0) = \langle (\Delta N)^2 \rangle \equiv \langle N^2 \rangle - \langle N \rangle^2. \quad (23b)$$

Here, μ and κ_T are, respectively, the chemical potential and the isothermal compressibility. The diffusion denominator reduces to the square of the particle number fluctuation in the system (at least for the selected form of the trial left eigenvector of the rate matrix in this work). Consequently, in a standard factorization of the collective diffusion coefficient,^{1,2,19}

$$D(\theta) = D_J(\theta) \left(\frac{\partial(\mu/k_B T)}{\partial \ln \theta} \right)_T, \quad (24)$$

we recognize in $N/\mathcal{N}(k=0)$ the static or thermodynamic factor, while the rate diffusion coefficient $D_J(\theta)$ (known as the kinetic factor) is then directly related to the numerator $\mathcal{M}(k)$:

$$D_J(\theta) = N^{-1} \lim_{k \rightarrow 0} \mathcal{M}(k)/k^2, \quad (25)$$

which has to be minimized with respect to the variational parameters.

We note in passing that it is not the main goal of this paper to provide another proof of the factorization embodied in Eq. (24). This was done several times in the past, starting from phenomenological considerations provided by Reed and Ehrlich¹ through their kinetic derivation²⁵ followed by Zhdanov's strict derivation^{19,26} based on mesoscopic considerations. It is, however, quite amusing that two mathematically abstract factors emerging from a variational approach to the eigenproblem of the rate matrix describing kinetics of microstates of the lattice gas, i.e., the norm of the trial eigenvector $\mathcal{N}(k)$ and the matrix expectation value $\mathcal{M}(k)$, are directly related to the collective diffusion coefficient thermodynamic and kinetic factors, respectively. This was not anticipated and, only recently,¹¹ clearly spelled out for a special case of diffusion in a lattice gas with long-range interparticle interactions.

1. Diffusion numerator $\mathcal{M}(k)$

The starting point is Eq. (18). The restriction that no linked pair of configurations ($\{m\}, \{m'\}$) may appear more than once in the sum is easily met if we allow, in the summation, only terms in which $W_{\{m\}, \{m'\}}$ is a rate of jump in the clockwise direction (i.e., jumps to the right). We consider one term or the sum of terms in which the particle executing the jump is not the reference particle—its initial position is, say, S_ℓ . This means $F_{\{m\}, \{m'\}}(k) = 1$, and we consider the factor $|\tilde{\phi}_{\{m'\}} - \tilde{\phi}_{\{m\}}|^2$. According to Eq. (21), almost all terms added together in $\tilde{\phi}_{\{m'\}}$ are identical to those in $\tilde{\phi}_{\{m\}}$ except for (i) the contribution due to the particle hopping from S_ℓ to $S_{\ell+1}$, (ii) the contribution due to a particle residing at $S_{\ell-1}$, and (iii) the contribution due to a particle residing at $S_{\ell+2}$. Of course, $\tilde{\phi}_{\{m'\}}$ and $\tilde{\phi}_{\{m\}}$ contain the latter two only if there is a particle at $S_{\ell-1}$ and/or $S_{\ell+2}$. Consequently, all phase contributions cancel out in the difference, leaving only the difference of at least one and at most three phase factors. Let us denote by $n_\ell = 0$ or 1 the occupation number of site S_ℓ and by $W_{\ell+1}^\ell(n_{\ell-1}, n_{\ell+2})$ the jump rate from site S_ℓ to $S_{\ell+1}$ which

depends on the potential well depth at S_ℓ , the height of the barrier to its right, and, on account of interactions, on the occupation of sites $S_{\ell-1}$ and $S_{\ell+2}$.

To provide an example, we consider the transition

$$\cdots \cdots \bullet_{(\ell-1)} \bullet_{(\ell)} \rightarrow \circ_{(\ell+1)} \circ_{(\ell+2)} \cdots \cdots \quad (26)$$

where the dots represent sites which are either occupied or empty and whose phase contributions to $\tilde{\phi}_{\{m'\}}$ and $\tilde{\phi}_{\{m\}}$ are the same. The hopping s th particle in configuration $\{m'\}$ resides at a site S_ℓ within unspecified elementary cell, and site $S_{\ell-1}$ is occupied and $S_{\ell+1}$ and $S_{\ell+2}$ are not. Only phases associated with these two particles change as the result of the jump. The jump rate is $W_{\ell+1}^\ell(1, 0)$, and in $|\tilde{\phi}_{\{m'\}} - \tilde{\phi}_{\{m\}}|^2$, only phase factors associated with sites $S_{\ell-1}$, S_ℓ , and $S_{\ell+1}$ are different in $\tilde{\phi}_{\{m'\}}$ than they are in $\tilde{\phi}_{\{m\}}$. Consequently, $|\tilde{\phi}_{\{m'\}} - \tilde{\phi}_{\{m\}}|^2$ reads

$$\begin{aligned} & |e^{ika(m_s-1+\delta_{\ell-1}+\Delta_{\ell-1}^R)} + e^{ika(m_s+\delta_\ell+\Delta_\ell^L)} - e^{ika(m_s-1+\delta_{\ell-1})} \\ & - e^{ika(m_s+1+\delta_{\ell+1})}|^2 \rightarrow (ka)^2(1 - \delta_\ell + \delta_{\ell+1} - \Delta_{\ell-1}^R - \Delta_\ell^L)^2, \end{aligned} \quad (27)$$

where the arrow denotes the long wavelength limit. Note that the distance of the hopping particle from the reference atom (am_s) drops out of this result already before the limit is taken. The result holds also when the reference particle itself executes the jump.^{7,8} This means that there is a macroscopic number of contributions to Eq. (18) with identical combination of geometrical and correlational phases—the one like in Eq. (27). The geometrical phase $\delta_{\ell-1}$ associated with the particle immediately to the left of the hopping one drops out in the long wavelength limit. In Ref. 7, the four sites explicitly shown in Eq. (26) have been termed the *active cell*. Here, with several nonequivalent sites in an elementary cell, one must consider active cells centered on each of them [in the same sense as the active cell shown in Eq. (26) is centered on site S_ℓ]. Four possible occupation patterns of the cell result in modifications of a bare jump rate. Of course, interactions and phase correlations going beyond the nearest sites require larger active cells and accordingly increased number of their occupation patterns.

Having all this in mind, we can now write the general expression for $\mathcal{M}(k)$. We have

$$\mathcal{M}(k) = L(ka)^2 \sum_{\ell=0}^n \mathcal{W}_\ell, \quad (28)$$

where

$$\begin{aligned} \mathcal{W}_\ell &= W_{\ell+1}^\ell(0, 0) \langle hnhh \rangle_\ell (1 - \delta_\ell + \delta_{\ell+1})^2 + W_{\ell+1}^\ell(1, 0) \\ &\quad \times \langle nnhh \rangle_\ell (1 - \delta_\ell + \delta_{\ell+1} - \Delta_{\ell-1}^R - \Delta_\ell^L)^2 + W_{\ell+1}^\ell(0, 1) \\ &\quad \times \langle hnhn \rangle_\ell (1 - \delta_\ell + \delta_{\ell+1} + \Delta_{\ell+1}^R + \Delta_{\ell+2}^L)^2 + W_{\ell+1}^\ell(1, 1) \\ &\quad \times \langle nnhn \rangle_\ell (1 - \delta_\ell + \delta_{\ell+1} - \Delta_{\ell-1}^R - \Delta_\ell^L + \Delta_{\ell+1}^R + \Delta_{\ell+2}^L)^2. \end{aligned} \quad (29)$$

Here, $\langle \cdots \rangle_\ell$ denotes four-site correlation function evaluated with equilibrium probabilities $P_{\{m\}}^{\text{eq}}$. For example,

$$\langle hnhh \rangle_\ell = \langle (1 - n_{\ell-1})n_\ell(1 - n_{\ell+1})(1 - n_{\ell+2}) \rangle. \quad (30)$$

Only correlations involving four neighboring sites are needed. These correlations provide the dependence on coverage and temperature (the latter is also embedded in the rates). The number of variational parameters is quite large: n geometrical phases δ_ℓ (recall that $\delta_0=0$) and, in principle, $2(n+1)$ correlational ones. They enter into \mathcal{M} in a quite simple way and, in practice, the number of correlational phases can be significantly reduced if several sites within elementary cell are identical.

2. Diffusion denominator $\mathcal{N}(k)$

The diffusion denominator $\mathcal{N}(k)$ was evaluated for a homogeneous substrate in Refs. 7, 9, and 11 for several interaction models in 1D homogeneous substrates. Explicit calculation, based on a quite complicated combinatorics, is not very transparent but it was shown in Ref. 11 that for a homogeneous substrate with long-range interactions between the nearest particles, the diffusion denominator is given in the long wavelength limit by Eqs. (23). In fact, this is not accidental and can be demonstrated to hold for a non-homogeneous substrate with arbitrary interactions at least for the current choice of the trial left eigenvector of the rate matrix. The proof, interesting in its own right, is not essential for the application of the method so it is given in Appendix A. Here, we quote the result only,

$$\mathcal{N}(k) \xrightarrow{k \rightarrow 0} \langle (\Delta N)^2 \rangle = L \sum_{\ell, \ell'=0}^n \sum_{j=0}^{L-1} (\langle n_\ell^0 n_{\ell'}^j \rangle - \theta_\ell \theta_{\ell'}), \quad (31)$$

where $\langle (\Delta N)^2 \rangle = \langle N^2 \rangle - \langle N \rangle^2$ is the (quadratic) particle number fluctuation, $n_\ell^j(\{m\}) = 0, 1$ is the occupation number of site S_ℓ within j th elementary cell in the configuration $\{m\}$, and $\langle \dots \rangle$ denotes statistical equilibrium average using probabilities $P_{\{m\}}^{\text{eq}}$. Of course, $\theta_\ell = \langle n_\ell^j \rangle$ does not depend on j and the correlation is a periodic function of j and j' with period 1: $\langle n_\ell^j n_{\ell'}^{j'} \rangle = \langle n_\ell^0 n_{\ell'}^{j'-j} \rangle$. Standard thermodynamic relations between $\langle (\Delta N)^2 \rangle$ and the isothermal compressibility κ_T or $(\partial \theta / \partial \mu)_{T,L}$ give the result in Eq. (23a). Extracting from the sum in Eq. (31) terms with $\ell = \ell'$ and $j = 0$, we can write

$$\mathcal{N}(0) = L \sum_{\ell=0}^n \theta_\ell (1 - \theta_\ell) + L \sum_{\ell, \ell'=0}^n \sum_{j=0}^{L-1} (1 - \delta_{\ell, \ell'} \delta_{j,0}) (\langle n_\ell^0 n_{\ell'}^j \rangle - \theta_\ell \theta_{\ell'}). \quad (32)$$

Note that only two-site correlation functions are needed here, but in contrast to $\mathcal{M}(k)$, they can involve sites at any distance from each other.

For the noninteracting system for which $\langle n_\ell^0 n_{\ell'}^j \rangle = \langle n_\ell^0 \rangle \langle n_{\ell'}^j \rangle = \theta_\ell \theta_{\ell'}$ —except when $\ell = \ell'$ and $j = 0$ —the second term at the right-hand side of Eq. (32) disappears and we get

$$\mathcal{N}(0) = L \sum_{\ell=0}^n \theta_\ell (1 - \theta_\ell). \quad (33)$$

III. SIMPLE APPLICATION: NONINTERACTING SCHWOEBEL SYSTEM

We apply the results of Sec. II D to evaluate the collective diffusion coefficient for a noninteracting lattice gas migrating along a line with a Schwoebel potential barrier.^{20,21} An algebraic expression for $D(\theta)$ can be derived in this case. This example is relevant for diffusion on a surface with steps. Strictly speaking, the latter is a two-dimensional problem but, without interparticle interactions, the diffusion along steps and that across them (being of our primary interest here) can be considered separately and the resulting collective diffusion coefficient is a diagonal tensor in a coordinate system with coordinate axes directed along these two directions. Its first simple theoretical treatment by Butz and Wagner²⁷ was motivated by the observed anisotropy of Pd and Au diffusion on single crystal planes of tungsten. General theoretical formulation (which offers also a possibility of accounting for interactions) is due to Zhdanov²⁸ who applied the approach formulated earlier in Ref. 19. It was further generalized and numerical examples were provided by Pereyra *et al.*²⁶ Nonequilibrium diffusion on a stepped surface with various types of interparticle interactions was investigated recently using numerical simulation²⁹ (interacting case) and analytic³⁰ (noninteracting case) methods. The only theoretical attempt to date which offers a possibility of direct numerical comparison with our results, to be given at the end of Sec. IV, is due to Merikoski and Ying.^{22,23} It was motivated by diffusion experiments of CO on clean stepped surface of Ni(110).^{31–33} Such comparison is important because the methods in both approaches are entirely different: analytic mean-field approach using Green's function techniques, on one hand, and the variational eigenvalue problem for the rate matrix, on the other hand. Note that interparticle interactions are accounted for in our general formulation, and discussion of such cases will be presented in the future.

In the Schwoebel system model, the “tagged” site S_0 binds a particle with different energy than all the remaining sites S_1, \dots, S_n , all of which have the same binding energy. Also, the tagged potential energy barrier height between sites S_n and S_0 is different than the barrier heights between all other sites being equal to each other. In the diagram in Eq. (2), the tagged barrier is at the position of the vertical bars representing boundaries of the elementary cell. The tagged site S_0 is immediately to its right.

When no other interactions between particles, except blocking preventing two particles to occupy the same site, are present, then there are only four distinct transition rates,

$$\overset{\circ}{W}_n^0 = W_L = \nu e^{-\beta(\delta E + \Delta + \delta E_B)},$$

$$\overset{\circ}{W}_0^n = V_R = \nu e^{-\beta(\Delta + \delta E_B)},$$

$$\overset{\circ}{W}_1^0 = W_R = \nu e^{-\beta(\delta E + \Delta)},$$

$$\overset{\circ}{W}_0^1 = V = \nu e^{-\beta \Delta},$$

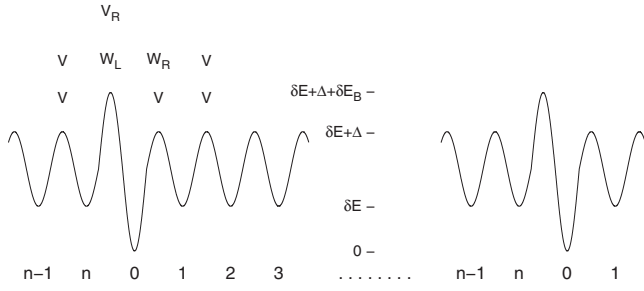


FIG. 1. Schwoebel barrier potential energy landscape. Only the S_0 adsorption site potential energy well depth and the potential energy barrier between S_n and S_0 sites are different from those for all remaining n sites and barriers within the elementary cell. Jump rates defined in Eq. (34) are shown. The Schwoebel barrier shown here corresponds to $r < 1$ and $\gamma > 1$.

$$\tilde{W}_{\ell+1}^{\ell} = \tilde{W}_{\ell}^{\ell+1} = V, \quad \ell = 1, 2, \dots, n-1. \quad (34)$$

The expressions at the right hand side of Eqs. (34) provide the standard Arrhenius parametrization of the rates in terms of the frequency prefactor ν , $\beta = 1/k_B T$, and potential energies at the bottom of the wells and the top of the barriers between them. By definition, $\Delta > 0$ and δE and δE_B must be such that the smallest of the activation energies present in the exponents is positive. The Schwoebel barrier potential energy landscape, energy scale, and the hopping rates are visualized in Fig. 1.

If μ is the chemical potential, then

$$\theta_0 = \langle n_0 \rangle = \frac{e^{\beta\mu}}{1 + e^{\beta\mu}}, \quad (35a)$$

$$\theta_x = \langle n_{\ell} \rangle = \frac{e^{-\beta(\delta E - \mu)}}{1 + e^{-\beta(\delta E - \mu)}}, \quad \ell = 1, 2, \dots, n-1 \quad (35b)$$

are the equilibrium occupation probabilities for, respectively, the tagged site S_0 and the remaining ones. The particle density (coverage) is then

$$\theta = \frac{\theta_0 + n\theta_x}{n+1}. \quad (36)$$

There are two distinct detailed balance conditions,

$$\begin{aligned} V\theta_x(1 - \theta_0) &= W_R\theta_0(1 - \theta_x), \\ V_R\theta_x(1 - \theta_0) &= W_L\theta_0(1 - \theta_x), \end{aligned} \quad (37)$$

which allow us to introduce two dimensionless system parameters,

$$\gamma = \frac{W_R}{W_L} = \frac{V}{V_R} = e^{\beta\delta E_B}, \quad (38a)$$

$$r \equiv \frac{\theta_x(1 - \theta_0)}{\theta_0(1 - \theta_x)} = \frac{W_R}{V} = \frac{W_L}{V_R} = e^{-\beta\delta E}. \quad (38b)$$

Note that r fully determines the equilibrium properties of the system; in fact, the first term at the right hand side of Eq. (38b) is just a ratio of two possible two-site equilibrium cor-

relation functions. For $r=1$, the potential well depths of all sites are the same (then $\delta E=0$, $W_R=V$, $W_L=W_R=W$, and $\gamma = V/W$). When the tagged S_0 site has a potential well deeper than the remaining sites, then $r < 1$, as shown in Fig. 1. The parameter γ , on the other hand, depends on the difference δE_B of the potential barrier heights encountered by the particle leaving the S_n or S_0 site hopping to the left or right. This parameter does not enter any equilibrium physical quantities but it is important for kinetics. For $\gamma=1$, potential barrier heights between any neighboring sites are the same ($\delta E_B = 0$, $V_R=V$, $W_L=W_R=W$, and $r=W/V$). The tagged barrier higher than all remaining ones, shown in Fig. 1, corresponds to $\gamma > 1$. Another case of interest is $r=\gamma$ corresponding to $\delta E_B = -\delta E$ and $W_L=V$. In such case, the S_0 well bottom and the barrier top to its left are raised ($r=\gamma > 1$) or lowered ($r=\gamma < 1$) with respect to all the remaining ones by the same amount. Consequently, all jumps to the left occur at the same rate V , while the particle hopping to the right does it at a rate V for any jump except when it crosses the barrier after two jumps: one of them occurring at a higher and the other at a lower rate than V .

The numerator $\mathcal{M}(k)$ is obtained from Eqs. (28) and (29) after observing that for the noninteracting case, the correlations factorize; for example, the correlation in Eq. (30) reads

$$\langle n_h n_{h+1} n_{h+2} \rangle_{\ell} = (1 - \langle n_{\ell-1} \rangle) \langle n_{\ell} \rangle (1 - \langle n_{\ell+1} \rangle) (1 - \langle n_{\ell+2} \rangle), \quad (39)$$

with θ_0 and θ_x eventually replacing the occupation number expectation values according to Eq. (35).

The diffusion coefficient denominator depends only on the equilibrium properties for which the parameter γ is irrelevant. For the noninteracting system, we get, from Eq. (33)

$$\mathcal{N}(0) = L[\theta_0(1 - \theta_0) + n\theta_x(1 - \theta_x)]. \quad (40)$$

The collective diffusion coefficient is obtained by evaluating

$$D(\theta) = \frac{\mathcal{M}}{\mathcal{N}(0)k^2}, \quad (41)$$

in which the size of the system cancels out.

A. Simple case: $n=1$

To get the feeling of the procedure involved, we consider first the $n=1$ case. Here, $\ell=0, 1$, and we have two sites with different potential well depths per elementary cell. The height of the barrier at each side of each cell is different. The rates are the first four listed in Eq. (34) and $\langle n_0 \rangle = \theta_0$ and $\langle n_1 \rangle = \theta_x$. There is only one geometrical phase, δ_1 (recall that $\delta_0=0$ by definition), and four correlational phases, Δ_0^R , Δ_0^L , Δ_1^R , and Δ_1^L . There are only two contributions to $\mathcal{M}(k)$, \mathcal{W}_0 and \mathcal{W}_1 in which the correlational phases appear only through the following sums:

$$\begin{aligned} \Delta_1^R + \Delta_0^L &\equiv \Delta_{10}, \\ \Delta_0^R + \Delta_1^L &\equiv -\Delta_{01}. \end{aligned} \quad (42)$$

From Eq. (29), we get

$$\mathcal{W}_0 = V\theta_x(1-\theta_0)\{(1-\theta_x)(1-\theta_0) + \theta_x\theta_0\}(1+\delta_1)^2 + \theta_x(1-\theta_0)(1+\delta_1-\Delta_{10})^2 + (1-\theta_x)\theta_0(1+\delta_1+\Delta_{10})^2\}, \quad (43a)$$

$$\mathcal{W}_1 = V[\theta_x(1-\theta_0)/\gamma]\{(1-\theta_x)(1-\theta_0) + \theta_x\theta_0\}(1-\delta_1)^2 + \theta_0(1-\theta_x)(1-\delta_1+\Delta_{01})^2 + (1-\theta_0)\theta_x(1-\delta_1-\Delta_{01})^2\}. \quad (43b)$$

Minimizing with respect to δ_1 , Δ_{01} , and Δ_{10} results in three linear equations for these parameters which yield

$$\delta_1 = \frac{1-\gamma}{1+\gamma}, \quad (44a)$$

$$\Delta_{01} = \frac{r-1}{r+1}(1-\delta_1), \quad (44b)$$

$$\Delta_{10} = \frac{r-1}{r+1}(1+\delta_1). \quad (44c)$$

Substituting back to \mathcal{W}_ℓ 's, one gets, after some algebra,

$$\mathcal{M}(k) = \frac{4LVr(ka)^2}{(r+1)(\gamma+1)}[\theta_0(1-\theta_0) + \theta_x(1-\theta_x)], \quad (45)$$

which, with \mathcal{N} given in Eq. (40), results in the coverage independent collective diffusion coefficient

$$D = Va^2 \frac{4r}{(r+1)(\gamma+1)}, \quad n=1. \quad (46)$$

This is a remarkably simple result: With blocking interactions only, the diffusion coefficient for the two-well-two-barrier Schwoebel barrier system does not depend on coverage, exactly like in a lattice with one type of wells and barriers. Note that this is not the exact result but merely the best variational approximation presently possible. It is encouraging that the same result is obtained exactly for $\theta=0$ and $\theta=1$ when one considers a random walk of a single particle or single hole on the two-well-two-barrier Schwoebel barrier lattice.

B. General $n \geq 3$

For the correlational phases needed in Eq. (29), the symmetry property

$$\Delta_1^R = \Delta_2^R = \cdots = \Delta_{n-1}^R = \Delta \neq 0, \quad (47)$$

$$\Delta_2^L = \Delta_3^L = \cdots = \Delta_n^L = -\Delta$$

leads to cancellations of all of them. The only correlational phases which remain are Δ_0^R , Δ_0^L , Δ_n^R , and Δ_1^L , but they enter into the final results only as sums,

$$\Delta_n^R + \Delta_0^L \equiv \Delta_{n0}, \quad (48)$$

$$\Delta_0^R + \Delta_1^L \equiv -\Delta_{01}.$$

We get (recall $\delta_0=0$)

$$\mathcal{W}_0 = V\theta_x(1-\theta_0)[(1-\theta_x)(1+\delta_1)^2 + \theta_x(1+\delta_1-\Delta_{n0})^2],$$

$$\mathcal{W}_1 = V\theta_x(1-\theta_x)[(1-\theta_0)(1-\delta_1+\delta_2)^2 + \theta_0(1-\delta_1+\delta_2+\Delta_{01})^2],$$

$$\mathcal{W}_l = V\theta_x(1-\theta_x)(1-\delta_l+\delta_{l+1})^2, \quad l=2,3,\dots,n-2,$$

$$\mathcal{W}_{n-1} = V\theta_x(1-\theta_x)[(1-\theta_0)(1-\delta_{n-1}+\delta_n)^2 + \theta_0(1-\delta_{n-1}+\delta_n+\Delta_{n0})^2],$$

$$\mathcal{W}_n = (V_R/\gamma)\theta_x(1-\theta_0)[(1-\theta_x)(1-\delta_n)^2 + \theta_x(1-\delta_n-\Delta_{01})^2]. \quad (49)$$

Equation (37) was used to replace $W_R\theta_0(1-\theta_x)$ with $V\theta_x(1-\theta_0)$ in \mathcal{W}_0 and V_R with V/γ in \mathcal{W}_n .

Note that we have ended up with $n+2$ variational parameters: δ_ℓ for $\ell=1,2,\dots,n$, Δ_{n0} , and Δ_{01} . Adding all above results [cf. Eq. (28)] and minimizing \mathcal{M} , we obtain $n+2$ linear equations for these parameters. The set can be solved for general $n \geq 3$. Details can be found in Appendix B. Cases $n=0$ (trivial, noninteracting case), $n=1$, and $n=2$ must be treated separately (no expressions for the latter; surprisingly complicated cases are given in this paper). For $n \geq 3$, expressions for all phases are quite involved and can be easily deduced from the results listed in Appendix B.

The diffusion coefficient, obtained from Eq. (41) using \mathcal{N} and $\mathcal{M}(k)$ from, respectively, Eqs. (40) and (B8) is

$$D(\theta) = Va^2 \frac{(1-\theta_x)(\theta_0+\theta_x)}{\theta_0(1-\theta_0) + n\theta_x(1-\theta_x)} \times \frac{r(n+1)^2}{(1+\gamma)(r+\gamma)F + (n-1)(r+1) + (n-3)(r-1)\theta_0}, \quad (50)$$

where

$$F = \frac{\Delta_{01}}{\gamma\Delta_{n0}} = \frac{\theta_0+\theta_x}{\gamma\theta_0+\theta_x}. \quad (51)$$

It is worthwhile to list the results for the diffusion coefficient for $\theta \rightarrow 0$ (single particle migration) and $\theta \rightarrow 1$ (single hole migration). They are obtained setting $e^{\beta\mu} \ll 1$ and $e^{\beta\mu} \gg 1$, respectively, in Eq. (35) before using the results in Eq. (50). The result is

$$D(\theta=0) = Va^2 \frac{r(n+1)^2}{(\gamma+n)(rn+1)}, \quad (52a)$$

$$D(\theta=1) = Va^2 \frac{r(n+1)^2}{(n+r)[1+\gamma+r(n-1)]}. \quad (52b)$$

Both results are *exact* and can be derived from the rate equations describing hopping of an isolated particle or hole on a lattice shown in Fig. 1.⁵ Note that for $r=\gamma$, i.e. $\delta E = -\Delta E_B$ —c.f. Fig. 1—we get $D(0)=D(1)$. This is easy to understand: the rates of hops of an isolated particle (V , V_R and W_R) are equal to the rates of hops of an isolated hole in the opposite direction.

1. Special case: $n \gg 1$

For $n \gg 1$, we expect that different well depths at the tagged site and different barrier heights at the tagged barrier should not matter. Indeed, in this limit, we get from Eq. (50) the coverage independent collective diffusion coefficient

$$D = Va^2, \quad n \gg 1, \quad (53)$$

expected for the noninteracting lattice gas on a homogeneous substrate. Effectively, the influence of the Schwoebel barrier is overwhelmed by that due to all remaining identical barriers and sites.

2. Special case: All site wells of equal depths

When the well depths at all sites, including that of S_0 , are the same (but the potential barrier height of a tagged barrier between S_n and S_0 is still different from that of the others), then

$$\dot{W}_0^n = \dot{W}_n^0 = W,$$

$$\dot{W}_{\ell+1}^\ell = \dot{W}_\ell^{\ell+1} = V, \quad \ell = 0, 1, 2, \dots, n-1, \quad (54)$$

which means that the jump rate across the tagged barrier in either direction is $W = V_R = W_L$ while that across any other one is V (i.e., $W_R = V$). According to Eqs. (34) and (38b), we have $r=1$, and the only parameter of the system is γ which, from Eq. (38a), becomes

$$\gamma = \frac{V}{W}. \quad (55)$$

Equilibrium occupation probabilities of each site are the same,

$$\theta_x = \theta_0 \equiv \theta. \quad (56)$$

Substituting this in Eq. (50) results in the diffusion coefficient

$$D = Va^2 \frac{n+1}{n+\gamma}, \quad r=1, \quad (57)$$

which does not depend on coverage. In this case, both $\mathcal{N}(0)$ and $\mathcal{M}(k)$ are proportional to $\theta(1-\theta)$ exactly like for a homogeneous substrate (for which $r=\gamma=1$).

3. Special case: All barriers of equal heights

Another interesting special case is that of the tagged site S_0 having the well depth different from all others but the potential barrier height of the tagged barrier between S_n and S_0 being the same as that of all other barriers. The hopping rate out of the tagged site is denoted W while that out of any other site is V :

$$\dot{W}_1^0 = \dot{W}_n^0 = W,$$

$$\dot{W}_{\ell+1}^\ell = \dot{W}_{\ell-1}^\ell = V, \quad \ell = 1, 2, 3, \dots, n. \quad (58)$$

Consequently, $\gamma=1$, and the only system parameter is

$$r = \frac{\theta_x(1-\theta_0)}{\theta_0(1-\theta_x)} = \frac{W}{V}. \quad (59)$$

The diffusion denominator \mathcal{N} is given in Eq. (40), while the substitution of $\gamma=1$ into Eq. (B8) results in

$$\mathcal{M}(k) = L(ka)^2 V \theta_x (1-\theta_x) \frac{(n+1)^2(1+\sigma\theta_0)}{(n+1)+\sigma\theta_0(n-3)}, \quad (60)$$

where

$$\sigma = \frac{r-1}{r+1} = \frac{W-V}{W+V}. \quad (61)$$

The resulting diffusion coefficient is

$$D(\theta) = Va^2 \frac{\theta_x(1-\theta_x)}{\theta_0(1-\theta_0) + n\theta_x(1-\theta_x)} \frac{(n+1)^2(1+\sigma\theta_0)}{(n+1)+\sigma\theta_0(n-3)}, \quad \gamma=1, \quad (62)$$

from which, for $r=1$, we recover $D=Va^2$ in agreement with the $\gamma=1$ limit of Eq. (57).

IV. DISCUSSION AND NUMERICAL EXAMPLES

Before presenting numerical results, several general remarks are worth noting. Recall first that while the results for $D(\theta)$ [Eq. (50) for $n \geq 3$ and (46) for $n=1$] are approximate variational results which may possibly overestimate the true diffusion coefficient, the results in Eqs. (52) for $\theta=0$ and $\theta=1$ are confirmed by an independent calculation to be exact.

In particular, the coverage independence of the diffusion coefficient for $n=1$ [two nonequivalent adsorption sites, Eq. (46)] is plausible in view of the fact that the hopping rates (W_R, W_L, V_R, V) for an isolated particle are isomorphic with those for an isolated hole resulting in $D(\theta=0)=D(\theta=1)$. It is, of course, possible that the true diffusion coefficient is, for $\theta \neq 0$ and $\theta \neq 1$, lower than its end values but the variational result that it, in fact, does not depend on coverage is quite likely.

Another prediction is that for $r=1$, i.e., when the potential energy well depths of all adsorption sites are the same, the diffusion coefficient does not depend on coverage too [Eq. (57)]. This result is, again, highly plausible due to symmetry between the kinetics of an isolated hole with respect to that of an isolated particle for such a potential energy landscape. The presence of a tagged barrier higher than all the remaining ones ($\gamma > 1$) slows down the diffusive dissipation of density fluctuations in comparison with that for a homogeneous substrate resulting in $D < Va^2$. Tagged barrier lower than the remaining ones ($\gamma < 1$) has the opposite effect. Therefore, Eq. (57) confirms intuitive expectations.

In order to consider possible behaviors of $D(\theta)$ systematically, we summarize the cases investigated in the (r, γ) parameter space in Fig. 2. The thick continuous line, $\gamma=(3r-1)/(r+1)$, separates the space into two regions: that for which $D > Va^2$ and that for which $D < Va^2$, for $n=1$. For parameters r and γ on this line, the $n=1$ Schwoebel barrier system behaves, as far as the collective diffusion is concerned, like a homogeneous substrate system. The potential

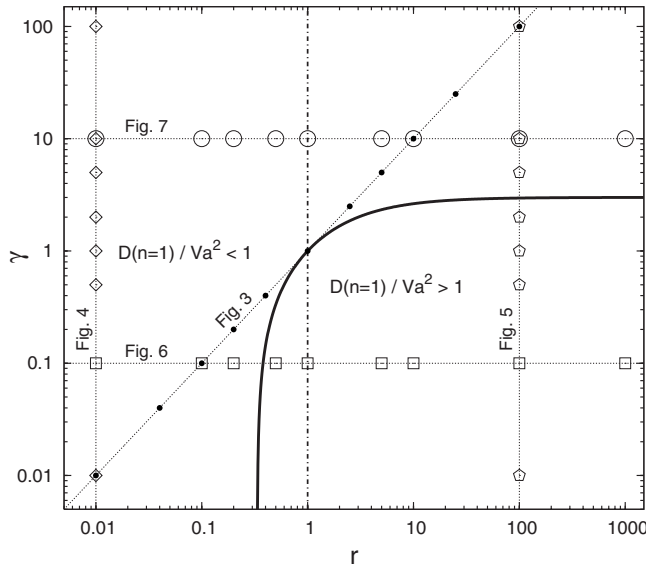


FIG. 2. Parameter space. Continuous: the $\gamma=(3r-1)/(r+1)$ line separating region in which $D(n=1)/Va^2 < 1$ from the one in which $D(n=1)/Va^2 > 1$. Dashes with dots: the $r=1$ line along which D does not depend on θ . Points on dotted lines correspond to $D(\theta)$ curves to be found in figures to follow as indicated.

energy modifications at the tagged well and the tagged barrier are such that their influences compensate each other so the line is from now on referred to as the *compensation line* [note that, in principle, r and γ depend on temperature, cf. Eq. (38), so the compensation is possible at one particular temperature only]. Another line of interest (dashes with dots) is that of $r=1$ for which the diffusion coefficient is coverage independent for any n . Note that for any n , according to Eq. (57), $D < Va^2$ above the compensation line along this line and $D > Va^2$ below the boundary, so, at least for $r=1$, the compensation line preserves its meaning also for $n \neq 1$. The remaining lines in Fig. 2 (fine dots) are labeled with Figs. 3–7. Points along these lines identify parameter pairs (r, γ) for which $D(\theta)$ are plotted in respective figures [i.e., $(r=0.1, \gamma=0.1)$ is plotted in both Figs. 3 and 6, while $(r=0.01, \gamma=0.1)$ is plotted in Fig. 6 but not in Fig. 4].

We consider first the case of $V=W_L$ which corresponds to $\gamma=rW_R/V=V/V_R$. Here, the potential energy at the bottom of the tagged well is modified with respect to all remaining wells by the same amount as the energy at the tagged barrier is modified with respect to all other barriers. As seen at the right hand side of Fig. 3, both the tagged barrier and the tagged well have lower (higher) energy than all the remaining ones when $r=\gamma < 1$ ($r=\gamma > 1$). For $\theta \approx 0$, the isolated particle hops between sites along the substrate from the right to the left at rate V even when it encounters the Schwoebel barrier (the tagged well and the tagged barrier): $\cdots \leftarrow V \leftarrow V \leftarrow V \leftarrow V \leftarrow V \cdots$. When it travels to the right, the hopping rates are also normally V except when it hops over the tagged barrier at rate V_R and then jumps out of the tagged well (traveling to the right) at rate W_R : $\cdots \rightarrow V \rightarrow V \rightarrow V_R \rightarrow W_R \rightarrow V \rightarrow V \cdots$. Concentrating on $\gamma=r < 1$, we have $W_R < V < V_R$, i.e., the first of the two Schwoebel barrier crossing jumps is relatively faster and the second one is relatively

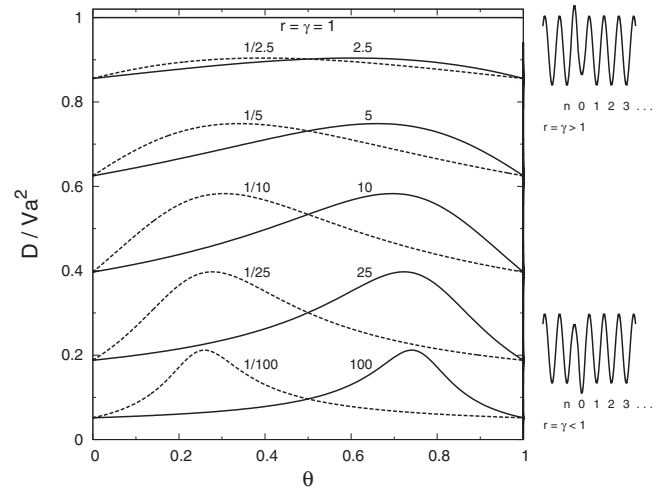


FIG. 3. Coverage dependence of the collective diffusion coefficient for several choices of $r=\gamma$ for $n=3$ demonstrating the particle-hole symmetry $D(\theta; r, \gamma=r) = D(1-\theta; 1/r, \gamma=1/r)$. Potential energy profiles at the right hand side correspond to cases $r=\gamma > 1$ and $r=\gamma < 1$ relevant to the data in the diagram. For each case, the potential energy is modified by the same amount at the tagged well bottom as it is at the corresponding hopping barrier.

slower than the “normal” rate V . For $\theta \approx 1$, we have to consider hops of isolated holes. Now, every jump of a hole to the right occurs at the same rate V , $\cdots \rightarrow V \rightarrow V \rightarrow V \rightarrow V \rightarrow V \rightarrow V \cdots$, while the hole hopping to the left (normally hopping at rate V) crosses the Schwoebel barrier in two consecutive jumps, the slower first (rate W_R) followed by the faster (rate V_R) one: $\cdots \leftarrow V \leftarrow V \leftarrow V_R \leftarrow W_R \leftarrow V \leftarrow V \cdots$. To have the situation completely analogous to that for $\theta=0$ (faster jump followed by the slower one), we must replace $r \rightarrow 1/r$, so $D(\theta=0; r=\alpha, \gamma=\alpha) = D(\theta=1; r=1/\alpha, \gamma=1/\alpha)$. Inverting both r and γ (while keeping them equal to each other) is equivalent to the particle-hole transformation. On the other hand, merely changing the order of the slow and the fast

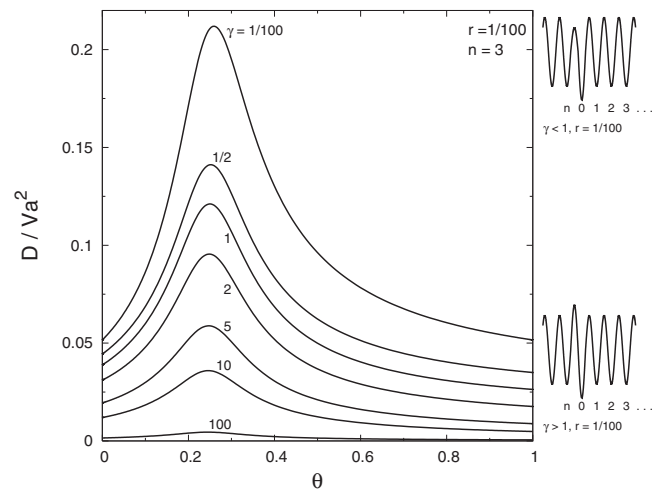


FIG. 4. Coverage dependence of the collective diffusion coefficient for systems with a deep tagged well ($r < 1$) for high ($\gamma > 1$, bottom curves) and low ($\gamma < 1$, top curves) tagged barriers.

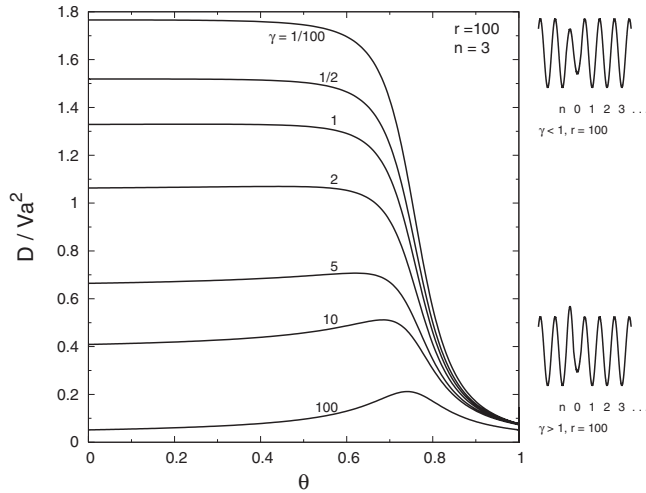


FIG. 5. The same as in Fig. 4 but for systems with a shallow tagged well ($r > 1$).

jumps does not affect the diffusion coefficient due to the migration of the isolated particles or holes, so we also have $D(\theta=0; r, \gamma=r) = D(\theta=1; r, \gamma=r)$. Both these relations are consistent with Eqs. (52).

For $\theta \neq 0, 1$, when the site blocking matters, the diffusion coefficient is expected to depend on that which of the two Schwoebel barrier crossing jumps is faster. The particle-hole transformation now reads $D(\theta; r=\alpha, \gamma=\alpha) = D(1-\theta; r=1/\alpha, \gamma=1/\alpha)$. Our algebraic result in Eq. (62) is expected to obey this symmetry, but proving it analytically is a very tedious and nontrivial task. We see, however, in Fig. 3 that it is perfectly obeyed. In fact, the curves for $\gamma=r=\alpha < 1$ can be perfectly superimposed on the corresponding curves for $\gamma=r=1/\alpha > 1$ by plotting them, respectively, as a function of θ and of $1-\theta$ on the same plot.

For $\gamma \neq r$, the diffusion coefficient does not exhibit the particle-hole symmetry. Algebraically, this can be seen from Eqs. (52) but can also be seen by examining what the hop-

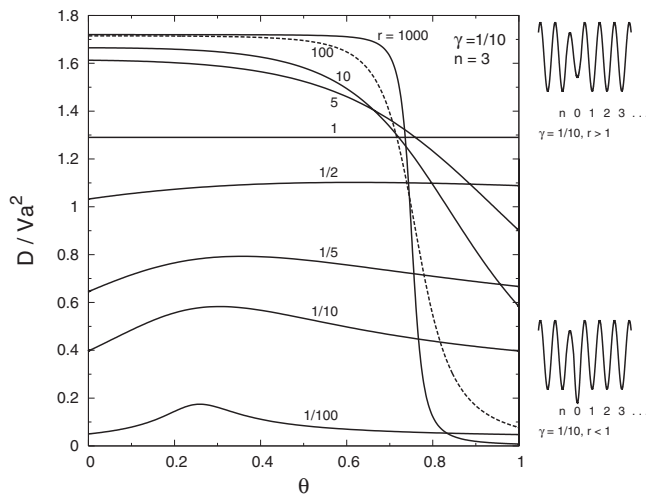


FIG. 6. Coverage dependence of the collective diffusion coefficient for systems with low tagged barrier ($\gamma < 1$) for deep ($r < 1$, bottom curves) and shallow ($r > 1$, top curves) tagged wells.

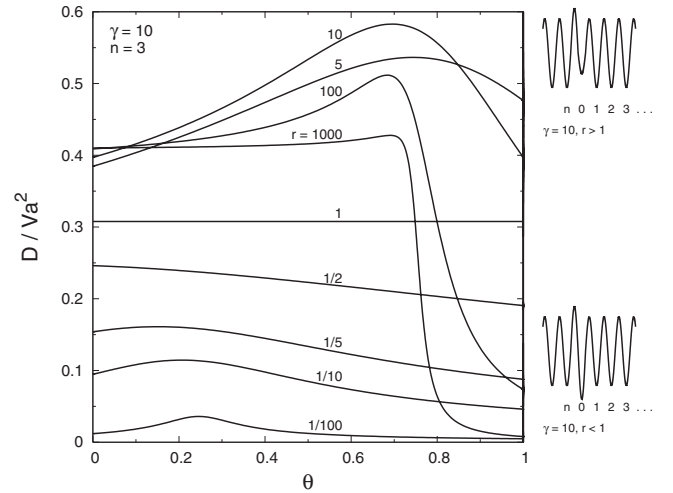


FIG. 7. The same as in Fig. 6 but for systems with high tagged barrier ($\gamma > 1$).

ping rates of an isolated particle are and comparing them with the hopping rates of an isolated hole. They are not related to each other by a simple ($W_R \leftrightarrow W_L, V_R \leftrightarrow V$) transformation, because away from the Schwoebel barrier, both the isolated particle and the isolated hole jump at the same rate V . Therefore, it is convenient to consider possible behaviors of $D(\theta)$ by varying either γ or r , keeping one of the parameters fixed.

We start with varying γ for $r = \text{const}$. The diffusion coefficient does not depend on coverage for $r=1$, so to see some interesting behavior, we choose r differing from 1 quite substantially (r depends exponentially on temperature and/or the well depth modification, so large deviations of r from 1 are not unrealistic). We choose $r=1/100$ (Fig. 4) and $r=100$ (Fig. 5). As seen from Fig. 2, varying γ (i.e., varying the height of the tagged potential energy barrier), we do not cross the compensation line in the former but cross it in the latter case. Indeed, the character of $D(\theta)$ and of its changes with varying γ are different in both figures. We have $D(\theta) < Va^2$ for all coverages for $r=0.01$ (Fig. 4), while for $r=100$ (Fig. 5), the diffusion coefficient becomes larger than Va^2 (for coverages up to $\theta \approx 0.7$) once the compensation line is crossed when γ is lowered below 3.

Slowing down diffusion for all coverages for $r < 1$ in comparison with the diffusion in a homogeneous substrate system may be understood on intuitive grounds. The tagged well is deeper than all remaining ones ($\delta E > 0$, cf. diagrams at right in Fig. 4), and at low temperatures, this well is occupied with a high probability even at low coverages by a particle which is difficult to kick out from this position. It, therefore, blocks other particles from wandering outside the elementary cells in which they initially are. Consequently, it takes more time for any density fluctuation to dissipate. Lowering γ facilitates kicking out particles from the tagged well, so in Fig. 4, the diffusion coefficient is generally larger for smaller γ but, still, it is unable to approach the homogeneous substrate limit. We know already from Eq. (53) that it approaches it only for $n \gg 1$, i.e., when the blocking at the tagged well, although still present, becomes irrelevant. Note

that the diffusion coefficient reaches maximum at a coverage $\theta \approx 1/(n+1) = 1/4$, which, in equilibrium, corresponds to the situation in which all particles present in the system are trapped in deep potential wells of the tagged sites. This behavior was already noted by Merikoski and Ying^{22,23} in their analytic mean-field approach using Green's function techniques.

For $r=100$ (Fig. 5), the behavior of the diffusion coefficient is dramatically different from that for $r < 1$. Here, the depth of the tagged site well is smaller than that of all other sites, so there is no blocking of particle migration by the tagged site at low coverages, particularly when γ is smaller than about 3 (i.e., below the compensation line along line labeled Fig. 5 in Fig. 3. In this region of the parameter space the height of the tagged barrier is either below that of all other barriers ($\gamma < 1$) or it exceeds them (for γ up to about 3) in the degree insufficient to induce an effective blocking at the Schwoebel barrier. Consequently, diffusion is more efficient than for a homogeneous substrate system, $D(\theta) > Va^2$, for coverages up to about 0.7. In fact, D is almost coverage independent in this coverage interval. For higher coverages, the diffusion coefficient drops sharply down to values well below that for the homogeneous substrate system. This can be rationalized as the result of blocking migration of holes by holes trapped at low temperatures at the bottom of the tagged well. In fact, the $r \gg 1$ limit $D(\theta=1) \rightarrow Va^2(n+1)^2/r(n-1) \rightarrow 0$ [cf. Eq. (52b)] can be understood exactly in the same way.

For γ above the compensation line, the diffusion coefficient drops below Va^2 for all coverages and develops a peak at $\theta \approx 1 - 1/(n+1) = 3/4$ corresponding, in thermal equilibrium, to the situation in which all tagged sites are unoccupied (filled with holes).

In Fig. 6, we examine $D(\theta)$ along the $\gamma=0.1$ line in Fig. 2. For r 's to the right of the compensation line (r larger than about $1/3$), the character the coverage dependence in Fig. 6 is similar to that already seen in Fig. 5 for $\gamma < 1$: flat plateau at $D=Va^2$ followed, for still larger r 's by its sharp drop. For $r=1000$, the coverage dependence of D is almost steplike. From Eqs. (50), we get $D(\theta=0) \rightarrow Va^2(n+1)^2/n(\gamma+n)$ for $r \gg 1$ and $D(\theta=1) \rightarrow (n+1)^2/r(n-1) \rightarrow 0$ for $r \gg 1$, γ . The observed $r=1000$ behavior is a precursor of an $r \rightarrow \infty$ limit easily deduced from Eq. (50): For $\theta < n/(n+1)$, the shallow tagged wells are unoccupied [i.e., $\theta_0=0$, $\theta_x=\theta(n+1)/n$], resulting in $D(\theta)=Va^2(n+1)^2/n(\gamma+n)=16Va^2/3(3+\gamma)$. For $\theta > n/(n+1)$, all deep wells are occupied [$\theta_x=1$, $\theta_0=\theta(n+1)-n$], resulting in a sudden drop of $D(\theta)$ to 0 at $\theta=n/(n+1)=3/4$.

Note that for r between about $r=1/3$ and $r=1$, we have rare cases with $D(\theta=1) > D(\theta=0)$, but $D(\theta)$ vary with θ very little here. For r below about $1/3$, we are in the region to the left of the compensation line in Fig. 2. Accordingly, $D(\theta) < Va^2$ for all coverages, with a maximum around $\theta=1/(n+1)=1/4$. As before, inefficient diffusion is due to the efficient blocking by particles trapped at the bottom of the tagged site well.

Finally, for $\gamma=10$ presented in Fig. 7, we never cross the compensation line in Fig. 2. Consequently, $D(\theta) < Va^2$ for all coverages. For $r \ll 1$, we again have the same behavior as

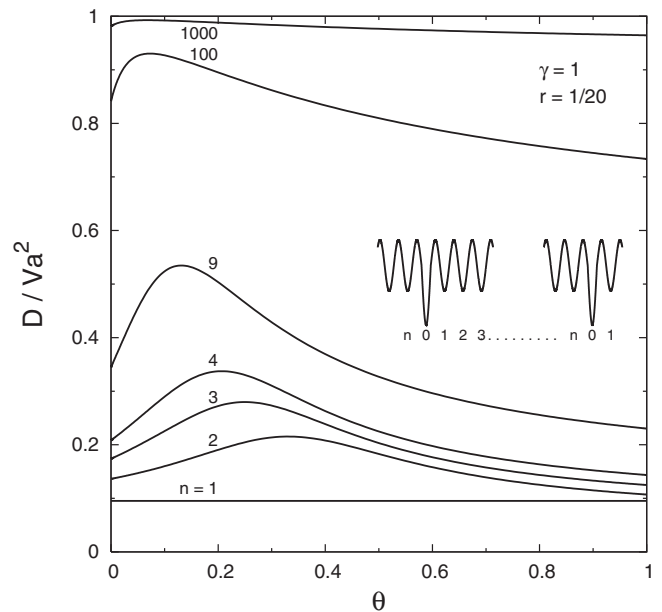


FIG. 8. Coverage dependence of the collective diffusion coefficient for different n .

that seen in Figs. 4 and 6 [a maximum around $\theta=1/(n+1)=1/4$]. For the tagged well shallower than the remaining ones ($r > 1$), $D(\theta)$ (still lower than Va^2) develops a maximum for $\theta > 1/2$ but then, for $r \rightarrow \infty$, it tends toward the steplike behavior between $D(\theta < n/(n+1)) = Va^2(n+1)^2/n(\gamma+n) < Va^2$ and $D(\theta > n/(n+1)) = 0$ discussed already. Note that for $r=5$, we again have a rare case of $D(1) > D(0)$.

All the numerical examples in Figs. 3–7 are for $n=3$, i.e., systems in which there are three “regular” sites for each tagged one. For $n \gg 1$, the diffusion coefficient tends, according to Eq. (53), to the homogeneous substrate limit $D=Va^2$ because the influence of the Schwoebel barrier is then overwhelmed by that due to regular barriers and sites. In Fig. 8, we present the coverage dependence of the diffusion coefficient for several values of n . For $n=1$, its coverage independent value, according to Eq. (46), is $D=4Va^2r/(r+1)(\gamma+1)=2Va^2r/(r+1) < Va^2$ for $\gamma=1$. For $n=1000$, we are here close to the homogeneous substrate limit $D=Va^2$. Similarly, like in Fig. 4, the diffusion coefficient for a given n has a maximum at approximately $\theta=1/(n+1)$, but this is not the exact rule and is already violated for $n=100$.

Monte Carlo simulations for the Schwoebel barrier system have been performed using the method described in Refs. 34 and 35, which allow us to determine the coverage dependence of the collective diffusion coefficient over the complete coverage interval from the results of a single numerical simulation. The Schwoebel barrier system presents a formidable challenge exactly because different locations along the substrate may effectively block the particle hopping and result in very long times before local thermal equilibrium is reached. Consequently, $D(\theta)$ with a prominent narrow peak like that seen in Fig. 4 is particularly difficult to simulate. Results of simulations for a few systems are presented in Fig. 9 and compared with the analytic theoretical

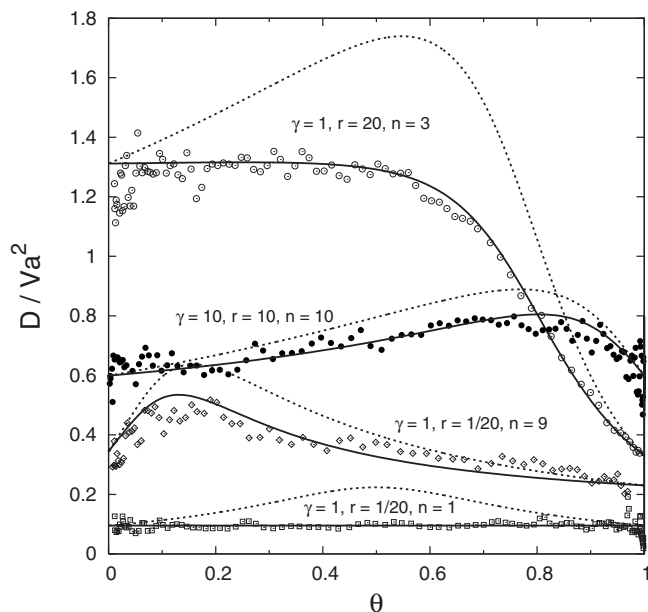


FIG. 9. Coverage dependence of the collective diffusion coefficient: Eq. (50), continuous; mean-field approximation of Ref. 23, Eq. (63), dashes; Monte Carlo simulations, points.

result for parameters listed there. Each type of behavior of $D(\theta)$ discussed so far is represented. The analytic results for $n=1$ and 9 are the same as in Fig. 8. The following key results of our theory are confirmed: (i) coverage independence for $n=1$, (ii) a maximum at $\theta \approx 1/(n+1)$ when $r < 1$ (cf. $n=9$ case), and (iii) a diffusion coefficient plateau for $r > 1$ for coverages up to around $n/(n+1)=3/4$ followed by its steep decrease (cf. the $n=3$ case). Several more simulations, not as accurate as the ones presented in Fig. 9, have been performed yielding similar results.

Diffusion in a noninteracting adsorbate on a stepped surface, modeled by the Schwoebel barrier, was investigated by Merikoski and Ying^{22,23} in terms of Green's functions method in a mean-field approach. Their analytic result [Eq. (3.8) in Ref. 23] reads in our notation (after assuming identical intrinsic prefactor for each microscopic jump rate) as follows:

$$D_{MY}(\theta) = Va^2 \frac{r(n+1)^2}{[n+r(\theta_0/\theta_x)^2][(n-1)r+(1+\gamma)\theta_x/\theta_0]}. \quad (63)$$

It is used by the authors also for $n=1$. It should be directly compared with the result in Eq. (50) or with Eq. (46) for $n=1$. First of all, one can show that for $\theta=0$ and $\theta=1$, both approaches yield the same exact result. For intermediate coverages, the results differ (having in some cases also a different coverage dependence character). For $n=1$, Eq. (63) predicts D which does depend on coverage in contrast to our prediction in Eq. (46). The mean-field result of Ref. 23, Eq. (63), is plotted in Fig. 9 (dashes). There is no doubt that for $n=1$ (the lowest curve), the coverage independence of D is quite strongly supported by the simulation results. For the $\gamma=1$, $r=20$, $n=3$ case (topmost curve), the character of the

coverage dependence predicted by both theories is different and the simulations support the result of the variational approach. The same is true, even with a bit noisier simulation results, in the remaining two cases for which the character of $D(\theta)$ is similar in both theories.

The strongest argument, however, favoring the variational approach over the mean-field one is theoretical. One can check that the mean-field result for D of Ref. 23 is never smaller than that resulting from the variational approach: $D_{MY}(\theta) \geq D(\theta)$ (with equality occurring only for $\theta=0$ and 1). This is seen in all cases shown in Fig. 9. According to the Ritz principle, the true diffusion coefficient cannot exceed the variational result (i.e., it cannot lie above the continuous lines in Fig. 9). Consequently, the results in Eq. (50) [and in Eq. (46) for $n=1$] represent a better approximation of the true diffusion coefficient than Eq. (63) does. We note here that the only existing analytic approach to nonequilibrium diffusion for a noninteracting lattice gas on a stepped surface³⁰ overestimates in the equilibrium limit, as realized by the authors, the collective diffusion coefficient even more than Eq. (63) does (cf. Ref. 30 for the discussion of this point).

V. DIFFUSION WITH INTER-PARTICLE INTERACTIONS: PRELIMINARY REMARKS

The main goal of this work is to present the systematic variational approach, based on a kinetic lattice gas model, on the investigation the collective diffusion process. The example, diffusion in a noninteracting gas, was selected for the illustration purposes due to its simplicity and the possibility of carrying out all calculations analytically. Truly interesting application is that to the systems with interactions. Modifications are quite straightforward. The diffusion coefficient denominator $\mathcal{N}(0)$ is still given by Eq. (A10) or (23a) and requires an evaluation of two-site correlation functions for the interacting system. Four-site correlation functions are needed for the diffusion coefficient numerator $\mathcal{M}(k)$ [cf. Eqs. (28)–(30)]. Both types of correlations can be evaluated exactly using properly generalized transfer matrix method.³⁶ Moreover, limiting attention to the Schwoebel barrier problem with interactions, there are more than three different hopping rates of jumps to the right ($W_{\ell+1}^\ell$, for $\ell=n, 0$ and $\ell \neq n, 0$) which multiply the four-site correlations in Eq. (29). They depend not only on the type of the site from which the jump originates (i.e., on ℓ) but also on the occupation state of the sites nearest to it. In the simplest case, four different rates correspond to four different occupation patterns^{7,9,11} of sites closest to site ℓ from which the jump originate. This results in 12 different rates (or eight for $n=1$). Detailed balance conditions allow us to introduce several parameters analogous to γ (ratios of rates of jumps in opposite directions) and r [ratios of two four-site correlation functions rather than a ratio of two two-site correlations in Eq. (38b)]. For the Schwoebel barrier problem, we get four parameters of each type. Minimization allows us to express all geometrical and occupational phases in terms of these parameters. The algebra is rather formidable and tedious, but it can be done using any of the symbolic manipulation programs such as MATH-

EMATICA or MAPLE resulting in complicated but algebraic result for $D(\theta)$. This program is now being developed and will be reported soon.

VI. SUMMARY AND CONCLUDING REMARKS

We have developed in this paper a systematic approach on collective diffusion in lattice gases adsorbed on a non-homogeneous but periodic substrate. It utilizes a properly modified, for non-Hermitian matrices, variational Ritz principle to find the lowest (diffusive) eigenvalue of the rate matrix describing microscopic kinetics of the system. The resulting coverage dependent collective diffusion coefficient bounds the true one from above. Phases associated, in the diffusive eigenvector of the matrix, with each occupied site contain corrections related to the position of the site within the periodic elementary cell as well as corrections due to a possible presence of particles at neighboring sites. These corrections are treated as variational parameters minimizing the diffusive eigenvalue.

The method, applicable in general to interacting lattice gases, was applied here for the sake of illustration to a lattice gas without (except for site blocking) interactions confined to a one-dimensional stepped substrate modeled by a Schwoebel barrier. This is perhaps the simplest nontrivial system for which fully algebraic result of manageable complexity can be obtained. Extensive discussion of the coverage dependence of the collective diffusion coefficient $D(\theta)$ is provided. Even without interparticle interactions, the analytic result for the coverage dependent collective diffusion coefficient admits a surprisingly rich spectrum of behavior which can, however, be rationalized using intuitive physical arguments.

The results are compared with the results for $D(\theta)$ obtained from numerical simulations and with the results of an analytic mean-field theory approach.^{22,23} The results of the Monte Carlo simulations validate the variational approach to collective diffusion coefficient $D(\theta)$, which is also shown to be never larger than that obtained using the mean-field theory. Consequently, the diffusion coefficient obtained using the variational approach is a substantial improvement over the mean-field theory result.

Finally, a procedure to be used to apply the method to the interacting system is described. The work in this direction is in progress.

Another direction of possible area of future applications of the variational approach to collective diffusion is its use for genuinely two-dimensional systems. For the particular example of diffusion on a stepped surface without interactions, the diffusion problem along steps is mathematically separate from the one across them, diffusion is anisotropic, and the discussion provided in this work applies to the matrix element of the diffusion coefficient tensor which describes diffusion across the steps. In particular, sharp features in Figs. 4–7 due to effective blocking of sites at the step edges by particles or holes remain intact. With the interactions, however, the problem does not factorize and both matrix elements must be obtained together. In principle, the variational approach in such case can be formulated in a way

analogous to that described in this work, but in practice, it soon may become overwhelming due to a large number of active cell occupation patterns which have to be considered. In particular, the blocking at the step edge sites might become less effective in two dimensions with interactions than it is in two dimensions without them, but this is not at all certain considering the long wavelength character of the diffusion process. In any case, structural organization of the adsorbate taking place in two dimensions with interactions at finite temperatures may be a factor affecting the collective diffusion coefficient dependence on coverage more drastically than the edge site blocking is. In principle, such phase transformations are built into the equilibrium correlation functions which enter the theory but, an evaluation of these correlations is a formidable task in its own right. In fact, an attempt at an investigation of the collective diffusion in a lattice gas with strong repulsive interparticle interactions on a homogeneous square lattice substrate for coverages around $\theta=0.5$ was already made.⁸ The structural organization of the adsorbate was imposed rather than derived, and the variational parameters were guessed using physical arguments rather than being obtained by minimizing the diffusive eigenvalue. An agreement between the results of this approach and the results of Monte Carlo simulations, although not perfect, was as good as could be expected given very much oversimplified state of the theory.

ACKNOWLEDGMENTS

This work was partially supported by research grants from the Natural Sciences and Engineering Research Council of Canada (NSERC) (Z.W.G.) and from Poland's Ministry of Science and Higher Education (Grant No. N202 042 32/ 1171) (M.A.Z.-K).

APPENDIX A

We use Eqs. (19) and (21) to derive the general expression for $\mathcal{N}(k)$ in the limit $k \rightarrow 0$. To do that, we reexpress $\tilde{\phi}_{\{m\}}(k)$ in such a form in which the summation over particles is replaced with summation over all sites in the system. Before doing that, we note that only am_s can be, in Eq. (21), comparable with the entire size of the system \mathcal{AL} . For example, for the s th particle residing at site S_{ℓ_s} within j_s th elementary cell (counting from the $j_0=0$ cell in which the reference particle resides), we have

$$am_s = \mathcal{A}j_s + (\ell_s - \ell_0)a, \quad (\text{A1})$$

and the phase factor associated with this particle in Eq. (21) is

$$e^{ika[(n+1)j_s + (\ell_s - \ell_0) + \delta_{\ell_s} + \Delta_{\ell_s}]}, \quad (\text{A2})$$

where j_s can be any integer between 0 and $L-1$. In view of the periodic boundary condition (3), the limit $ka \rightarrow 0$ must be taken carefully. On the other hand, however, ℓ_s , ℓ_0 , δ_{ℓ_s} , and Δ_{ℓ_s} are small in comparison with $L\mathcal{A}$, so expansion in powers of $ka[(\ell_s - \ell_0) + \delta_{\ell_s} + \Delta_{\ell_s}]$ can be done at the very beginning of the calculation. Therefore, for the purpose of evalu-

ating $\mathcal{N}(k \rightarrow 0)$, we can approximate $\tilde{\phi}(k)$ as follows:

$$\tilde{\phi}_{\{m\}}(k) \approx \sum_{s=0}^{N-1} e^{ikAjs}, \quad (\text{A3})$$

where the $s=0$ term refers to the reference particle itself ($j_0=0$). Introducing $n_\ell^j(\{m\})=0, 1$, the occupation number of site S_ℓ in the j th elementary cell in the configuration $\{m\}$, we can write

$$\tilde{\phi}_{\{m\}}(k) = \sum_{\ell=0}^n \sum_{j=0}^{L-1} e^{ikAj} n_\ell^j(\{m\}), \quad (\text{A4})$$

which can be now used in Eq. (19):

$$\mathcal{N}(k) \approx \sum_{j,j'=0}^{L-1} \sum_{\ell,\ell'=0}^n e^{ikA(j-j')} \langle n_\ell^j n_{\ell'}^{j'} \rangle, \quad (\text{A5})$$

where

$$\langle n_\ell^j n_{\ell'}^{j'} \rangle = \sum_{\{m\}} P_{\{m\}}^{\text{eq}} n_\ell^j(\{m\}) n_{\ell'}^{j'}(\{m\}) \quad (\text{A6})$$

is the two-site correlation function satisfying the following conditions:

$$\langle n_\ell^j n_{\ell'}^{j'} \rangle = \langle n_\ell^0 n_{\ell'}^{j'-j} \rangle = \langle n_\ell^0 n_{\ell'}^{j'-j+L} \rangle. \quad (\text{A7})$$

Changing in Eq. (A5) the summation index j' to $r=j'-j$, splitting the sum over r into contribution due to $r < 0$ and that due to $r \geq 0$, changing the summation index in the former contribution from r to $r'=r+L$, renaming r' to r , and using Eq. (A7), we get

$$\mathcal{N}(k) \approx L \sum_{\ell,\ell'=0}^n \sum_{r=0}^{L-1} e^{-ikAr} \langle n_\ell^0 n_{\ell'}^r \rangle. \quad (\text{A8})$$

We cannot set $k=0$ in this result yet because the correlation tends to a finite limit $\langle n_\ell^0 \rangle \langle n_{\ell'}^0 \rangle$ for large r . Replacing, however, $\langle n_\ell^0 n_{\ell'}^r \rangle$ with $(\langle n_\ell^0 n_{\ell'}^r \rangle - \langle n_\ell^0 \rangle \langle n_{\ell'}^0 \rangle) + \langle n_\ell^0 \rangle \langle n_{\ell'}^0 \rangle$ and using

$$\sum_{r=0}^{L-1} e^{-ikAr} = 0, \quad (\text{A9})$$

following from Eq. (3), we can set $k=0$ in the result, getting

$$\mathcal{N}(0) = L \sum_{\ell,\ell'=0}^n \sum_{r=0}^{L-1} (\langle n_\ell^0 n_{\ell'}^r \rangle - \langle n_\ell^0 \rangle \langle n_{\ell'}^0 \rangle). \quad (\text{A10})$$

Starting now from

$$N = \sum_{\ell=0}^n \sum_{j=0}^{L-1} n_\ell^j(\{m\}) \quad (\text{A11})$$

to evaluate the quadratic particle number fluctuation $\langle (\Delta N)^2 \rangle = \langle N^2 \rangle - \langle N \rangle^2$ and following the procedure identical to that used to get Eq. (A8) from Eq. (A5), we get for $\langle (\Delta N)^2 \rangle$ the expression at the right hand side of Eq. (A10). This completes the proof that $\mathcal{N}(0) = \langle (\Delta N)^2 \rangle$, and following from it, Eq. (23a) is generally valid.

APPENDIX B

The procedure and partial results contained in this appendix are valid for $n > 3$. Equating to zero the derivatives of $\mathcal{M}(k)$, given in Eqs. (28) and (49), with respect to δ_ℓ , $\ell = 1, 2, \dots, n$, Δ_{n0} , and Δ_{01} , one gets $n+2$ linear equations for these parameters. Among them, $n-4$ equations,

$$(1 - \delta_{\ell-1} + \delta_\ell) - (1 - \delta_\ell + \delta_{\ell+1}) = 0,$$

for $\ell = 3, 4, \dots, n-2$, allow us to find $\delta_4, \delta_5, \dots, \delta_{n-1}$ in terms of δ_2 and δ_3 ,

$$\delta_\ell = -\delta_2(\ell-3) + \delta_3(\ell-2), \quad \ell = 4, 5, \dots, n-1. \quad (\text{B1})$$

The remaining six equations can be dealt with most conveniently when five auxiliary parameters x_i defined through

$$\delta_1 = x_1 - 1,$$

$$\delta_2 = x_1 + x_2 - 2,$$

$$\delta_3 = x_1 + x_2 + x_3 - 3,$$

$$\delta_{n-1} = 2 - x_n - x_0,$$

$$\delta_n = 1 - x_0 \quad (\text{B2})$$

are introduced. This, together with Δ_{n0} and Δ_{01} , results in seven, rather than six, unknowns. The equations which they satisfy are

$$x_1 r \theta_0 - x_2 \theta_x - (r \Delta_{n0} + \Delta_{01}) \theta_0 \theta_x = 0,$$

$$x_2 - x_3 + \Delta_{01} \theta_0 = 0,$$

$$x_3 - x_n - \Delta_{n0} \theta_0 = 0,$$

$$x_n \theta_x - x_0 \frac{r}{\gamma} \theta_0 + \left(\Delta_{n0} + \frac{r}{\gamma} \Delta_{01} \right) \theta_0 \theta_x = 0,$$

$$-x_1 r + x_n + \Delta_{n0}(1+r) = 0,$$

$$x_2 - x_0 \frac{r}{\gamma} + \Delta_{01} \left(1 + \frac{r}{\gamma} \right) = 0. \quad (\text{B3})$$

This set allows us to express all x_i 's in terms of Δ_{n0} and Δ_{01} [Eq. (38b) is used to get the result],

$$x_0 = \gamma x_2 = \frac{r+\gamma}{r-1} \Delta_{01},$$

$$x_1 = x_n = \frac{r+1}{r-1} \Delta_{n0},$$

$$x_3 = \left(\frac{r+1}{r-1} + \theta_0 \right) \Delta_{n0}, \quad (\text{B4})$$

and to obtain the following relation between Δ_{n0} and Δ_{01} :

$$\Delta_{01}(\theta_x + \gamma\theta_0) = \Delta_{n0}\gamma(\theta_0 + \theta_x). \quad (\text{B5})$$

Another relation between Δ_{n0} and Δ_{01} is obtained from Eq. (B1) for $\ell=n-1$, which, in terms of x_i 's, reads

$$x_0 + x_1 + x_2 + x_n + (n-3)x_3 = n + 1, \quad (\text{B6})$$

after Eqs. (B2) are used in it. These two relations allow us to find Δ_{n0} :

$$\Delta_{n0} = \frac{(r-1)(n+1)}{(1+\gamma)(r+\gamma)F + (n-1)(r+1) + (n-3)(r-1)\theta_0}, \quad (\text{B7})$$

where F is defined in Eq. (51) from which Δ_{01} can also be deduced. Inserting all these solutions back into Eq. (49) results in

$$\mathcal{M}(k) = \frac{L(ka)^2 V r (1 - \theta_x)(\theta_0 + \theta_x)(n+1)^2}{(1+\gamma)(r+\gamma)F + (n-1)(r+1) + (n-3)(r-1)\theta_0}. \quad (\text{B8})$$

Although the procedure described in this appendix works for $n > 3$ only, some of the results quoted here including the result for $\mathcal{M}(k)$ hold also for $n=3$ but not for $n=1$ or 2.

*zalum@ifpan.edu.pl

†gortel@phys.ualberta.ca

¹D. A. Reed and G. Ehrlich, Surf. Sci. **102**, 588 (1981).

²R. Gomer, Rep. Prog. Phys. **53**, 917 (1990).

³A. Danani, R. Ferrando, E. Scalas, and M. Torri, Int. J. Mod. Phys. B **11**, 2217 (1997).

⁴T. Ala-Nissila, R. Ferrando, and S. C. Ying, Adv. Phys. **51**, 949 (2002).

⁵J. W. Haus and K. Kehr, Phys. Rep. **150**, 263 (1987).

⁶A. R. Allnatt and A. B. Lidiard, Rep. Prog. Phys. **50**, 372 (1987).

⁷Z. W. Gortel and M. A. Załuska-Kotur, Phys. Rev. B **70**, 125431 (2004).

⁸M. A. Załuska-Kotur and Z. W. Gortel, Phys. Rev. B **72**, 235425 (2005).

⁹Ł. Badowski, M. A. Załuska-Kotur, and Z. W. Gortel, Phys. Rev. B **72**, 245413 (2005).

¹⁰M. A. Załuska-Kotur, Ł. Badowski, and Z. W. Gortel, Physica A **357**, 305 (2005).

¹¹M. A. Załuska-Kotur and Z. W. Gortel, Phys. Rev. B **74**, 045405 (2006).

¹²W. Zwerger, Z. Phys. B: Condens. Matter **42**, 333 (1981).

¹³H. J. Kreuzer and J. Zhang, Appl. Phys. A: Solids Surf. **A51**, 183 (1990).

¹⁴H. J. Kreuzer, J. Chem. Soc., Faraday Trans. **86**, 1299 (1990).

¹⁵S. H. Payne and H. J. Kreuzer, Phys. Rev. B **75**, 115403 (2007).

¹⁶J.-S. McEwen, S. H. Payne, H. J. Kreuzer, and C. Bracher, Int. J. Quantum Chem. **106**, 2889 (2006).

¹⁷M. Yakes, M. Hupalo, M. A. Załuska-Kotur, Z. W. Gortel, and M. C. Tringides, Phys. Rev. Lett. **98**, 135504 (2007).

¹⁸A microstate representing a given equivalence class is termed a *configuration* in Refs. 7–11 and 17 and in the present work,

while in Ref. 16, it is referred to as a *primitive*.

¹⁹V. P. Zhdanov, Surf. Sci. **149**, L13 (1985).

²⁰R. L. Schwoebel and E. J. Shipsey, J. Appl. Phys. **37**, 3682 (1966).

²¹R. L. Schwoebel, J. Appl. Phys. **40**, 614 (1969).

²²J. Merikoski and S. C. Ying, Surf. Sci. **381**, L623 (1997).

²³J. Merikoski and S. C. Ying, Phys. Rev. B **56**, 2166 (1997); **58**, 15912 (1998).

²⁴R. Kutner, Phys. Lett. **81A**, 239 (1981).

²⁵D. A. Reed and G. Ehrlich, Surf. Sci. **105**, 603 (1981).

²⁶V. Pereyra, G. Zgrablich, and V. P. Zhdanov, Langmuir **6**, 691 (1990).

²⁷R. Butz and H. Wagner, Surf. Sci. **87**, 85 (1979).

²⁸V. P. Zhdanov, Phys. Lett. A **137**, 409 (1989).

²⁹M. Mašín, I. Vitulainen, T. Ala-Nissila, and Z. Chvoj, J. Chem. Phys. **122**, 214728 (2005).

³⁰Z. Chvoj, M. Mašín, and T. Ala-Nissila, J. Stat. Mech.: Theory Exp. **06**, P10003 (2006).

³¹X. D. Xiao, X. D. Zhu, W. Daum, and Y. R. Shen, Phys. Rev. B **46**, 9732 (1992).

³²X. D. Xiao, Y. Xie, and Y. R. Shen, Phys. Rev. B **48**, 17452 (1993).

³³X. D. Xiao, Y. Xie, C. Jakobsen, H. Galloway, M. Salmeron, and Y. R. Shen, Phys. Rev. Lett. **74**, 3860 (1995).

³⁴M. A. Załuska-Kotur, S. Krukowski, and Ł. A. Turski, Surf. Sci. **441**, 320 (1999).

³⁵M. A. Załuska-Kotur, S. Krukowski, Z. Romanowski, and Ł. A. Turski, Surf. Sci. **457**, 357 (2000).

³⁶R. J. Baxter, *Exactly Solved Models in Statistical Mechanics* (Academic, New York, 1982), Chap. 2.